LES ÉTUDES IN ISING FIELD THEORY AND RELATED PROBLEMS

BY

ISKANDER ZIYATDINOV

A dissertation submitted to the

Graduate School—New Brunswick

Rutgers, The State University of New Jersey

in partial fulfillment of the requirements

for the degree of

Doctor of Philosophy

Graduate Program in Physics and Astronomy

Written under the direction of

Alexander Zamolodchikov

and approved by

_____

_____

_____

_____

_____

New Brunswick, New Jersey

May, 2011

ABSTRACT OF THE DISSERTATION

LES ÉTUDES IN ISING FIELD THEORY AND RELATED PROBLEMS

by

ISKANDER ZIYATDINOV

Dissertation Director: Alexander Zamolodchikov

The main subject of this thesis is the Ising field theory, the field theory describing the scaling limit of the two-dimensional Ising model near its critical point. We study the Ising field theory in low- and high-temperature regimes.

In the low-temperature regime we address questions related to the mass spectrum of the bound states that exist in the theory. The overall goal is to study analytic properties of the masses taken as functions of the scaling variable in the theory. At this stage, we are primarily interested in the asymptotic series in the coupling parameter. We describe methods used for developing expansions in the coupling parameter when this parameter is sufficiently small. This gives rise to the low-energy and semiclassical series. Methods developed are then applied to a different model, a model that has many things in common with the Ising field theory, the two-dimensional quantum chromodynamics with infinite number of colors, also known as the 't Hooft model.

In the second part of the thesis we turn to the Ising field theory in the high-temperature regime. Here we study the problem of scattering in a weak magnetic field. We compute the leading perturbative correction to the scattering amplitude for the $2 \to 2$ process. This is done first by means of standard methods based on the direct

intermediate-state decomposition and dispersion relations. Then we compute the large energy asymptotic of the amplitude for this process directly using a known relation between the Ising field theory at zero magnetic field and classical sinh-Gordon equation. We obtain consistent results that show the logarithmic growth of the amplitude with energy at this order in magnetic field. Going beyond the leading order we argue that at large energies for a sufficiently weak magnetic field the amplitude exhibits a power-like decay.

Acknowledgements

I would like to express my deep gratitude to my advisor, Alexander Zamolodchikov, for his guidance. It has been a great privilege to work with him. His absolutely wonderful attitude about teaching and eternal patience are truly amazing.

I would like to thank my committee members, especially Gerald Goldin and Sergei Lukyanov, for illuminating discussions.

I owe a debt of gratitude to all professors at Rutgers for giving me a chance to learn from their wisdom. Among all, I would especially like to thank Ronald Ransome and Ted Williams for the support throughout my stay at Rutgers.

Special thanks go to Diane Soyak for making the life of the HET people as smooth as possible and to Shirley Hinds without whom the life of graduate students at the department would have stopped.

Table of Contents

List of Tables

List of Figures

Chapter 1

Introduction

Search for integrability is a common theme in physics. Discovery of every new integrable theory has always been followed by great advances in different areas of research including those at first sight completely unrelated. Conformal field theory in two dimensions is a classic example of such a process [1]. Soon after it appeared, it was shown that a very important class of conformal field theories known as "rational conformal field theories" is integrable, that there exists an infinite number of conserved charges which, in principle, allows to determine all there is to know about the theory. Interestingly, most of universality classes important in two-dimensional statistical mechanics are associated with rational conformal field theories. Subsequent development of conformal field theory has brought new ideas and methods in areas ranging from solid state physics to string theory.

Unfortunately, integrability is not always present. Most field theories are either non-integrable at all or almost integrable with a certain degree of carefully hidden integrability, and all known genuinely different integrable theories are easily countable. Moreover, integrabilty is known to be a very fragile property: in the presence of a generic deformation, the integrability is usually destroyed which makes studying the resulting deformed theory an unsurmountable task. At the same time, it was shown in [5] that there exist certain deformations, the so-called integrable deformations, that preserve integrability and allow to solve the theory non-perturbatively. Combined with methods of factorized S-matrices [6], this approach proved to be immensely useful in studying off-critical models[1]. For an arbitrary deformation, when the integrability is lost, the most common method to approach such deformed systems is to develop perturbation theory

[1] A thorough review of these matters can be found in, e.g., [7].

near integrable points, which, due to difficulties in constructing a general analytical framework, is usually implemented via numerical calculations [4, 8, 9, 10, 11, 12, 13, 14].

The Ising field theory (IFT), the main subject of this dissertation, serves a representative example of a phenomenon when the theory easily integrable at its critical point becomes more or less untreatable away from it except for special situations corresponding to the cases that can be interpreted in terms of integrable deformations in the above mentioned sense. To define what this theory is we first have to introduce another model, the model that gives rise to the IFT.

Consider the following model. Take a lattice with N nodes, and in each node place a variable σ_i, the "spin", taking values ± 1. With a given configuration (see one possible

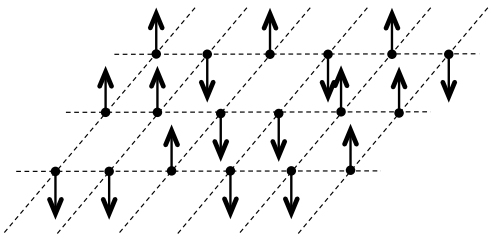

Figure 1.1: A possible spin configuration on a two-dimensional square lattice.

configuration on a two-dimensional square lattice in Fig. 1.1) we associate the energy

$$E[\sigma] = -J \sum_{\langle i,j \rangle} \sigma_i \, \sigma_j - H \sum_i \sigma_i, \tag{1.1}$$

where the sum in the interaction term goes over the neighboring spins only; J and H characterize the interaction of spins with each other and with the external magnetic field H, respectively. With this at hand, we can define the free energy of the model

$$f(H,T) = -T \lim_{N\to\infty} \frac{1}{N} \log \sum_{\{\sigma\}} e^{-E[\sigma]/T}. \tag{1.2}$$

This model is known as the Ising model in the magnetic field. It was first introduced as an approximate description of magnetics, but with time it turned out to be very general describing a whole class of systems, the so-called Ising universality class, among which one could name lattice gases, binary alloys and many others.

Although one can study the Ising model in any dimensions, we will restrict ourselves to and will always imply the special case of two dimensions. It appears to be important for several reasons. Since Peierls [15] it has been known that in the absence of the magnetic field the Ising model possesses a non-trivial phase structure with two distinct phases separated by a second-order phase transition (Fig. 1.2). In the low-temperature phase the symmetry with respect to the change of magnetization is broken and the phase is ordered, whereas in the high-temperature phase this symmetry is restored. Later on, this semiquantitative picture has been proven in the classic work by Onsager [16], who solved the 2D Ising model at $H = 0$ exactly.

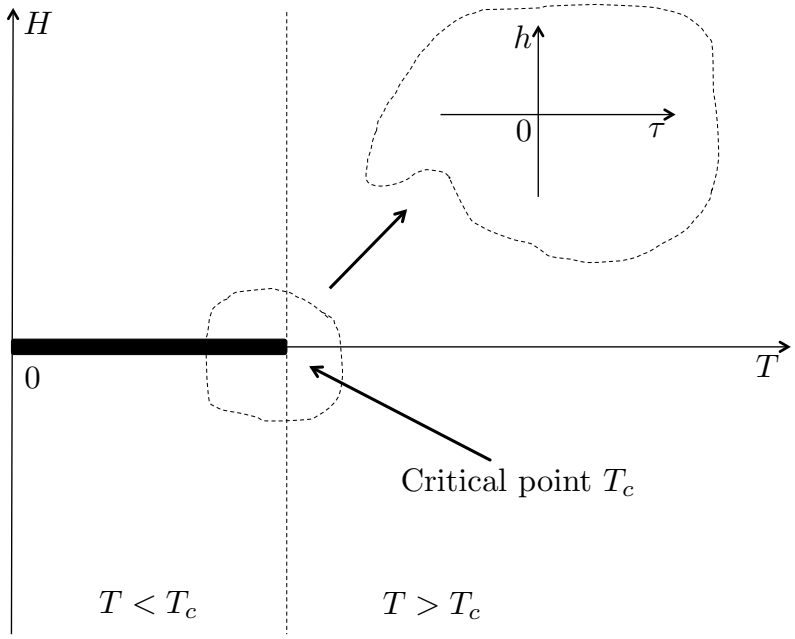

Figure 1.2: Phase diagram of the Ising model. The highlighted area represents the phase diagram of the Ising field theory.

Another reason of why the 2D Ising model is relevant is that in the scaling limit around its critical point $T = T_c$, $H = 0$, it is described by a certain field theory, which happens to be the simplest rational conformal field theory, the so-called $c = 1/2$ conformal field theory, deformed by both relevant operators present in the theory. To make this equivalence more clear, we should go back to the free energy of the Ising

model (1.2) and notice that it can be written as the sum of the regular part and the part that will contain all the singularities that define the phase structure of the model,

$$f(H,T) = f_{sing}(H,T) + f_{reg}(H,T). \tag{1.3}$$

It turns out that the leading singular part of $f_{sing}(H,T)$ is universal, it does not depend on the microscopic details of the formulation of a given model such as the properties of the original lattice or the physics of the model, with this information hidden in the sub-leading parts of $f_{sing}(H,T)$ and regular part $f_{reg}(H,T)$. What is more important is that this leading singular part can be interpreted as a vacuum energy density of a certain field theory, the IFT, which appears, despite the simplicity of its formulation, to be extremely rich in phenomena and proves to be an enormous challenge for studying.

In field-theoretic terms, the IFT is defined in terms of the Euclidean action[2]

$$\mathcal{A}_{\rm IFT} = \mathcal{A}_{c=1/2\ \rm CFT} + \tau \int \varepsilon(x)\ d^2x + h \int \sigma(x)\ d^2x \tag{1.4}$$

that represents a general renormalization group flow from the unitary conformal field theory with the central charge $c = 1/2$, given as a theory of free massless Majorana fermions, perturbed by its two relevant operators. The free fermion action can be written as

$$\mathcal{A}_{c=1/2\ \rm CFT} = \frac{1}{2\pi} \int \left(\psi\bar{\partial}\psi + \bar{\psi}\partial\bar{\psi}\right) d^2x, \tag{1.5}$$

where $x = (\mathrm{x}, \mathrm{y})$ are Euclidean coordinates, $\partial = \frac{1}{2}(\partial_{\mathrm{x}} - i\partial_{\mathrm{y}})$, $\bar{\partial} = \frac{1}{2}(\partial_{\mathrm{x}} + i\partial_{\mathrm{y}})$, ψ and $\bar{\psi}$ are chiral components of the Majorana fermion. The field $\varepsilon(x)$, of the conformal dimensions (1/2, 1/2), proportional to $\bar{\psi}\psi$ when written in terms of ψ and $\bar{\psi}$, represents the temperature deviation from the critical point, i.e., $\tau \sim (T_c - T)$, and is usually called as the "energy density". The "spin field" $\sigma(x)$ has the dimensions (1/16, 1/16), and the associated coupling parameter h is the rescaled magnetic field. Unlike the "energy density" operator, it does not have a simple form in terms of ψ and $\bar{\psi}$ [17]. We assume the following normalizations of these fields as $|x| \to 0$,

$$|x|^2 \langle \varepsilon(x)\, \varepsilon(0) \rangle \to 1, \quad |x|^{1/4} \langle \sigma(x)\, \sigma(0) \rangle \to 1.$$

[2]We will imply the analytical continuation, $\mathrm{y} \to i\mathrm{t}$, to the Minkowski space when required.

The parameters τ and h have mass dimensions 1 and 15/8, respectively. Thus, apart from the overall mass scale, the theory depends on a single dimensionless parameter η,

$$\eta = \frac{2\pi\tau}{|h|^{8/15}} \equiv -\frac{m}{|h|^{8/15}}, \tag{1.6}$$

with the parameter $m = -2\pi\tau$ introduced for later use[3].

The theory (1.4) admits an exact solution at a few special, "integrable", points. The first one, most obvious, is the case of zero magnetic field, $h = 0$. This integrable point is due to the presence of the exact solution of the Ising model on the lattice before the scaling limit is performed. In the continuous limit, at this point the IFT is equivalent to the field theory of free fermions with the mass $|m|$ theory (see, e.g., [2]). The phase structure of the theory in the continuous limit remains the same. If one expresses this point $\tau \neq 0$, $h = 0$ in terms of η as $\eta = \pm\infty$, then the two phases are differentiated by the sign of the infinity. At $\eta = +\infty$, i.e., in the low-T regime, the spin-reversal symmetry is spontaneously broken, and the field $\sigma(x)$ develops nonzero expectation value $\langle\sigma(x)\rangle = \pm\bar{\sigma}$, with $\bar{\sigma}$ known exactly [3]

$$\bar{\sigma} = |m|^{1/8}\,\bar{s}, \qquad \bar{s} = 2^{1/12}e^{-\frac{3}{2}\zeta'(-1)} = 1.35783834170660\ldots \tag{1.7}$$

At $\eta = -\infty$, i.e., in the high-T regime, the symmetry is restored and $\langle\sigma(x)\rangle = 0$. These regimes are related by a duality transformation. The second solvable point in the IFT is $\tau = 0$, i.e., $\eta = 0$, where the theory is no longer free, but the exact solution can still be obtained due to the presence of infinitely many local integrals of motion [5]. There is one more special point, the Lee-Yang point [18], which appears if one allows η to take complex values. To be more specific, at the Lee-Yang point, m takes real positive values and $h = \pm i\,a\,m^{15/8}$ with $a = 0.18933(2)$. These points are known to be critical [19], and the associated conformal field theory is the non-unitary minimal model with $c = -22/5$ [20].

These integrable points can be classified via renormalization group language. Thus the first case, when the resulting theory is the theory of free massive Majorana fermions,

[3]This parameter, m, or more precisely, $|m|$, is typically associated with the mass of elementary particles of the theory.

corresponds to the situation when the $c = 1/2$ conformal field theory is deformed by the "energy density" field. The second integrable point is the result of deforming the same conformal field theory with the "spin density" field. Finally, the Lee-Yang point corresponds to the deformation with a special combination of these two operators representing the renormalization group flow from the $c = 1/2$ conformal field theory to the $c = -22/5$ conformal field theory.

In a general case, away from the critical point $\tau = 0$, $h = 0$, at arbitrary values of η, the theory (1.4) is not integrable (see, e.g., [25]). It can be represented as a massive quantum field theory with interaction, and just like with any massive field theory, its physical content can be understood in terms of the spectrum of particles and their interactions, that is, their scattering amplitudes.

The particle content is qualitatively understood since [4]. As η changes, the spectrum of stable particles gradually changes from an infinite tower of "mesons", bound states of the elementary "quark" fields, in the low-T regime at $\eta \to +\infty$ to a single particle in the high-T regime with $\eta \to -\infty$. On quantitative level, various expansions of some of the masses near the integrable points are available through the perturbation theory [4, 8, 9, 10, 11, 12, 13, 14], and rather accurate numerical data were obtained in [8, 9] by means of the "truncated conformal space approach" of [21], and by numerical diagonalization of the lattice transfer-matrix [22, 23]. First few masses from the IFT spectrum as functions of η are shown in Fig. 1.3, obtained in [9], thus providing quantitative evidence to support the qualitative scenario of [4].

With regard to the problem of scattering, apart from the integrable points, there is little known about it. Analytic treatment is hampered by the apparent difficulty to develop conventional covariant perturbation theory for the IFT. As for the numerical approach, the methods of [21] turn out to be of limited power here. While these methods are successful in numerical evaluations of low-energy scattering phases [24], it is not clear how to apply them to the analysis of the the high-energy scattering. At the same time, understanding scattering amplitudes, in particular, their high-energy behavior, is essential — it can provide important insights into the structure of the theory. When the parameter η changes, some particles lose their stability becoming virtual or resonance

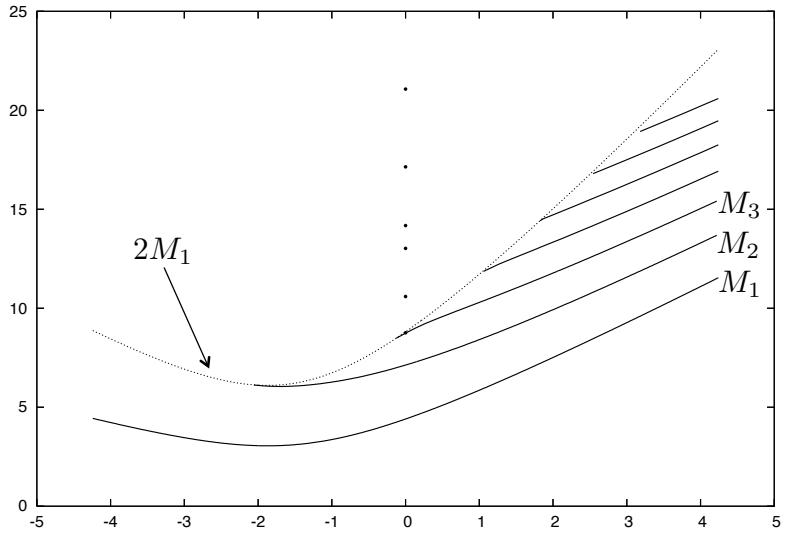

Figure 1.3: First few masses in the IFT spectrum as functions of η. The dotted line represents the lowest stability threshold $2M_1$. 8 points at $\eta = 0$ correspond to 8 stable particles existing due to the integrability of the IFT at $\eta = 0$.

states. Qualitative changes in the spectrum typically occur when the masses of some resonance states in units of the stable particle masses go to infinity. Analyzing this phenomenon clearly requires some knowledge about the high-energy scattering.

In this dissertation we attempt to address both topics, the analytic properties of the mass spectrum and the scattering. In the first part of the thesis (Chapter 2) we describe methods of studying the mesons' mass spectrum introduced in [13]. These methods are later used on a different model, the 2D QCD with infinite number of colors [36]. This theory appears to be very similar to, albeit simpler in some respects than the IFT. The goal of this analysis is twofold: firstly this model represents an interesting problem by itself, and secondly it serves a sort of a litmus test for the technique.

In the second part of the thesis (Chapter 3) we study the $2 \to 2$ scattering in the high-temperature IFT [41]. Our analysis is based on the perturbation theory developed around the integrable point $\eta = -\infty$. The goal is to compute the first correction in h^2 to the scattering amplitude. At first, this is done by means of the intermediate-state decomposition that when combined with certain dispersion relations on the amplitude

makes it possible to compute the dominant contribution of the amplitude. Then we use a known relation between the IFT at $h = 0$ and the classical sinh-Gordon problem to compute the large-energy asymptotic of the standard perturbative matrix element directly. In the end of the chapter we also propose an approximation that allows us to derive the large-energy asymptotic of the scattering amplitude beyond the leading order in h^2.

Chapter 2

Mass spectrum in two-dimensional theories with confinement. Low-temperature Ising field theory and 't Hooft model.

In this chapter we describe methods that are used to study the particle spectrum in the IFT and apply them to the problem of the bound states in the 't Hooft model.

As it was mentioned in the introduction, the IFT at zero magnetic field in the low-T regime can be described a theory of Majorana fermions of mass m. These fermions can be interpreted as domain walls between spatial domains of positive and negative magnetization. Switching on a weak magnetic field provides confining interaction of the form $h \int \sigma(x)\, dx$ [1] that makes it possible for fermions to form stable bound states, "mesons". The natural question that one can ask is about properties of masses of these mesons, how they behave when considered as functions of the scaling parameter η. The qualitative picture has been developed in [4]. According to this scenario, fermions, free at $\eta = +\infty$, become confined once η becomes finite, $\eta < \infty$. As η decreases, the heavier mesons become unstable and decay into the lighter ones, typically turning into resonances. With η nearing 0, some of resonances become stable again, this stability is related to the integrability of the IFT at $\eta = 0$ mentioned in the Introduction. As η decreases further, all particles but one disappear[2], and at $\eta = -\infty$ the IFT again becomes a theory of free fermions, the result expected from the duality.

In [9, 13] authors proposed to study the mass spectrum of bound states in the

[1] The appearance of this confining force can be understood as follows. In the low-temperature phase, σ develops non-zero vacuum expectation $\langle \sigma(x) \rangle = \bar{\sigma}$. Hence, two fermions located at x_1 and x_2 will interact according to the potential $V \approx 2\bar{\sigma} h\, |x_1 - x_2|$.

[2] In fact, already at $\eta < \eta_2 \approx -2.09$, seen in the Fig. 1.3, there will be just one stable particle left in the spectrum [9].

problem via the Bethe-Salpeter equation. Though written in a certain, rather limiting approximation, it gives a very good agreement with the qualitative scenario above.

Another theory, simpler in some respect (to be made clear below), exhibiting if not the same, then at least very similar properties is the so-called 't Hooft model. This name is given to the QCD in two dimensions with infinite number of colors, $N_c = \infty$ [26]. From the particle content point of view, the 't Hooft model and IFT are not very different, each being a two-dimensional theory of fermions with a confining interaction. Among many features of the model we will be interested in the following one: it is known since [26] that mesons and their spectrum can be exactly described in terms of solutions of a certain integral equation, again the Bethe-Salpeter equation. This equation, unlike the one suggested for the IFT, is exact at $N_c = \infty$. At the same time, 2D QCD with finite N_c, just like the IFT, is known to be non-integrable (see, e.g., [31]). This, together with the results of studies of the 't Hooft model, might give us some intuition as what to expect in the full IFT.

Although the Bethe-Salpeter equation in for the 't Hooft model can be solved numerically [28, 29, 30, 31], this equation, due its elegance and simplicity, deserves an analytical study. In particular, one is interested in analytic properties of the spectrum as functions of parameters of theory, that is, the coupling constant and masses of quarks, taken as complex variables. With this goal in mind, the authors of [35] proposed a novel method for studying analytic properties of solutions of the equation, more specifically the spectrum of the problem. Although they consider the case when quark masses have special values, the method they developed is general and many conclusions about properties of the spectrum are applicable or can be extended to a general case without any obvious difficulties.

In the following sections we outline the methods developed in [13] and apply them to the case of the 't Hooft model. The results of the analysis are then compared to the direct numerical solution of the problem.

2.1 Bethe-Salpeter equation in IFT

The qualitative picture of the interaction in the low-temperature IFT via a linear potential appears to be sufficient to give a rather good approximation for the bound-state masses. Thus, the theory is roughly equivalent to the problem of two interacting fermions described in terms of the Hamiltonian

$$\hat{H} = \omega(p_1) + \omega(p_2) + 2\bar{\sigma}h\,|\mathrm{x}_1 - \mathrm{x}_2| \tag{2.1}$$

with $\omega(p) = \sqrt{m^2 + p^2}$ being the energy of a particle with mass m and momentum p. This interpretation already turns out to be powerful enough to give the first terms in the asymptotic expansions of the meson masses in two extreme parts of the spectrum, the low-energy and semiclassical limits. For example, in the low-energy limit, that is, in the lower part of the spectrum, fermions can be treated as non-relativistic with $\omega(p) \approx m^2 + p^2/(2m)$, and the problem of studying the meson spectrum M_n is reduced to finding the eigenvalues of the Hamiltonian $p^2/m + 2\bar{\sigma}h\,|\mathrm{x}|$. Hence for the meson masses M_n one will have

$$M_n \approx 2m\left(1 + \frac{(2\bar{\sigma}h/m^2)^{2/3}}{2}\,z_n\right), \tag{2.2}$$

where z_n, $n = 1, 2, \ldots$, are consecutive zeroes of the Airy function $\mathrm{Ai}(-z)$. This result was first obtained through the analysis of the spin-spin correlation function in [4].

For the higher part of the spectrum, M_n with $n \sim m^2/(\bar{\sigma}h)$, one should use the semiclassical approximation. Classically, two fermions forming the meson can be treated as distinguishable particles moving between collisions towards each other under constant acceleration. To describe their motion it is convenient to work in the center-of-mass frame where the trajectories of both fermions can be parametrized in terms of a single variable, the rapidity θ, so that the two particles have the rapidities $+\theta$ and $-\theta$. The time along the trajectory is taken as $\mathrm{t} - \mathrm{t}_0 = R\sinh\theta$, where t_0 is a suitable reference time and $R = m/(2\bar{\sigma}h)$ is a characteristic spatial scale of the problem. Up to a permutation of the quarks, the coordinate along the trajectory within a cycle is then given as

$$\mathrm{x} \equiv \mathrm{x}_2 - \mathrm{x}_1 = 2R\,(\cosh\vartheta - \cosh\theta), \quad -\vartheta \le \theta \le \vartheta, \tag{2.3}$$

where ϑ is a parameter specifying the classical trajectory, and the momentum is

$$p \equiv \frac{p_1 - p_2}{2} = -m \sinh\theta. \tag{2.4}$$

The mass of the meson can be extracted as the center-of-mass energy associated with the trajectory, $M = 2m\cosh\vartheta$. The reduced action per cycle takes the form

$$\oint p\, d\mathrm{x} = 2\int_{-\vartheta}^{\vartheta} p\, d\mathrm{x} = 4mR\int_{-\vartheta}^{\vartheta} \sinh^2\theta\, d\theta = \frac{2(\sinh 2\vartheta - 2\vartheta)}{\lambda}, \tag{2.5}$$

where λ is the dimensionless ratio $2\bar{\sigma}h/m^2$. Hence, using the Bohr-Sommerfeld quantization condition $\oint p\, d\mathrm{x} = 2\pi(N + 1/2)$, $N = 0,\ 1,\ \ldots$, and taking into account the fermionic nature of quarks that prescribes N to be odd, $N = 2n - 1$, $n = 1,\ 2,\ \ldots$, one gets the quantization condition in the form

$$\sinh 2\vartheta_n - 2\vartheta_n = 2\pi\lambda(n - 1/4) \tag{2.6}$$

that leads to the WKB meson spectrum,

$$M_n = 2m\cosh\vartheta_n. \tag{2.7}$$

A more systematic approach, proposed in [9, 13], is developed under the assumption that in the low-T limit the Ising mesons can be considered mainly as two-quark constructs, which is true at a sufficiently weak magnetic field. Under this assumption it is possible to write down an equation, the Bethe-Salpeter equation, that allows to greatly improve on the simple qualitative interpretation. Here we will sketch the reasoning underlying its derivation.

We start from the integrable point $\eta = -\infty$, that is, when the magnetic field is zero. At this point the theory is described by the free Hamiltonian

$$\hat{H}_0 = E_0 + \int_{-\infty}^{\infty} \frac{dp}{2\pi}\, \omega(p)\, \hat{a}_p^\dagger \hat{a}_p, \tag{2.8}$$

where the creation-annihilation operators $\hat{a}_p$, $\hat{a}_p^\dagger$ are subject to the usual anticommutators, $\{\hat{a}_p, \hat{a}_q^\dagger\} = (2\pi)\,\delta(p - q)$, and together with the vacuum state they give the Fock space of states.

The magnetic field provides the interaction

$$\hat{H} = \hat{H}_0 + h\int_{-\infty}^{\infty} \sigma(x)\, d\mathrm{x}, \quad \sigma(x) \equiv \sigma(\mathrm{x}, \mathrm{t})|_{\mathrm{t}=0}\,. \tag{2.9}$$

The natural way is to approach the problem perturbatively. Unfortunately, it is not as straightforward as it seems: the difficulty in analyzing the spectrum of this hamiltonian is due to the fact the usual covariant perturbation theory is not available for the IFT. We are left to use the quantum-mechanical perturbation theory and make sure that at every step Lorentz co- and invariance can be restored. Nevertheless, one can proceed thanks to the fact that matrix elements of $\sigma(x)$ between the states with any number of fermions at $h = 0$ are known explicitly [27].

The eigenstates of the Hamiltonian (2.9) are of the form

$$|\Psi\rangle = |\Psi^{(2)}\rangle + \dots \tag{2.10}$$

where the two-quark component is

$$|\Psi^{(2)}\rangle = \frac{1}{2}\int \frac{dp_1}{2\pi}\frac{dp_2}{2\pi}\,\Psi(p_1,p_2)|p_1,p_2\rangle, \tag{2.11}$$

and $\dots$ stand for multi-particle contributions, present in general.

Hence, using the explicit expression for the $2 \to 2$ matrix element of $\sigma(x)$

$$G(p_1,p_2|q_1,q_2) = \frac{1}{4\sqrt{\omega(p_1)\omega(p_2)\omega(q_1)\omega(q_2)}}\left[\frac{\omega(p_1)+\omega(q_1)}{p_1-q_1}\frac{\omega(p_2)+\omega(q_2)}{p_2-q_2} - \right.$$
$$\left. - \frac{\omega(p_1)+\omega(q_2)}{p_1-q_2}\frac{\omega(p_2)+\omega(q_1)}{p_2-q_1} + \frac{p_1-p_2}{\omega(p_1)+\omega(p_2)}\frac{q_1-q_2}{\omega(q_1)+\omega(q_2)}\right], \tag{2.12}$$

we can rewrite the eigenvalue problem $\hat{H}|\Psi\rangle = E|\Psi\rangle$ in the two-quark approximation as

$$[\omega(p_1)+\omega(p_2)-\Delta E]\,\Psi(p_1,p_2) =$$
$$= f_0\int_{-\infty}^{\infty}(2\pi)\delta(p_1+p_2-q_1-q_2)\,G(p_1,p_2|q_1,q_2)\,\Psi(q_1,q_2)\,\frac{dq_1}{2\pi}\frac{dq_2}{2\pi}, \tag{2.13}$$

where $f_0 = 2\bar{\sigma}h$ is the "string tension", and $\Delta E = E - E_{vac}$ will be associated later on with the energy of a meson with the mass M and the momentum P, $\Delta E = \sqrt{M^2+P^2}$.

The meson is a bound state of two quarks, hence the wave function of the meson with the momentum P can be written as

$$\Psi(p_1,p_2) = (2\pi)\,\delta(p_1+p_2-P)\Psi_P(p_1-P/2), \tag{2.14}$$

and the equation (2.13) becomes

$$[\omega(P/2-p)+\omega(P/2+p)-\Delta E]\,\Psi_P(p) = f_0 \int\!\!\!\!\!\!-_{-\infty}^{\infty} G_P(p|q)\,\Psi_P(q)\,\frac{dq}{2\pi}, \tag{2.15}$$

where $G_P(p|q) = G(P/2+p, P/2-p|P/2+q, P/2-q)$. Here $\Psi_P(p)$ is assumed to be normalizable with the norm

$$\|\Psi_P\|^2 = \frac{1}{2\Delta E}\int_{-\infty}^{\infty} |\Psi_P(p)|^2\,\frac{dp}{2\pi}. \tag{2.16}$$

The kernel, $G_P(p|q)$, has the form

$$G_P(p|q) = \frac{1}{(p-q)^2} - \frac{1}{(p+q)^2} + G_P^{(reg)}(p|q). \tag{2.17}$$

One can notice that since the pole terms have the same effect as the linear potential above, this equation refines the earlier qualitative picture taking into account the short-range interaction $G_P^{(reg)}(p|q)$.

It appears that the most tractable version of the equation is obtained if one goes to the reference frame related to the meson with $P \to \infty$. Moreover, it has been argued that in this limit some of the corrections necessary to restore the Lorentz invariance, which is lost within this two-quark approximation, disappear[3].

Eventually, in this limit, using the parametrization in terms of the rapidity variable $\tanh\theta = 2p/P$, we get

$$\left(m^2 - \frac{M^2}{4\cosh^2\theta}\right)\Psi(\theta) = f_0 \int\!\!\!\!\!\!-_{-\infty}^{\infty} G(\theta|\theta')\Psi(\theta')\frac{d\theta'}{2\pi}, \tag{2.18}$$

where

$$G(\theta|\theta') = 2\,\frac{\cosh(\theta-\theta')}{\sinh^2(\theta-\theta')} + \frac{1}{4}\frac{\sinh\theta}{\cosh^2\theta}\frac{\sinh\theta'}{\cosh^2\theta'} \tag{2.19}$$

and $\Psi(\theta) = \lim_{P\to\infty}\Psi_P(p)$.

This equation (2.18) is referred as the IFT Bethe-Salpeter equation. It can be interpreted as the eigenvalue problem for the meson masses[4] M^2

$$\hat{H}\Psi = M^2\Psi \tag{2.20}$$

---

[3]Similar arguments were used in the context of the 't Hooft model in [32].

[4]One should mention that these values M^2 are not the actual meson masses due to the approximate nature of the equation. Nevertheless, in the weak-coupling limit they are sufficiently close. Unfortunately, due to the nature of the Bethe-Salpeter equation there is no parameter that controls the approximation.

with the Hamiltonian $\hat{H}$ defined as

$$\hat{H}\Psi(\theta) = 4\cosh^2\theta \left(m^2\Psi(\theta) - f_0 \fint_{-\infty}^{\infty} G(\theta|\theta')\Psi(\theta')\frac{d\theta'}{2\pi} \right) \tag{2.21}$$

and acting in the Hilbert space with the metric following from (2.16) in the form

$$\|\Psi\|^2 = \int_{-\infty}^{\infty} \frac{d\theta}{2\pi} \frac{|\Psi(\theta)|^2}{4\cosh^2\theta}. \tag{2.22}$$

In this metric $\hat{H}$ is Hermitian; moreover, it can be shown that its eigenvalues are not just real, but also positive.

For this Bethe-Salpeter equation one develops the weak-coupling expansion for the mesons masses taking the dimensionless combination $\lambda = f_0/m^2$ to zero, in other words, setting the string tension f_0 in units of m^2 be small. Depending on how one takes the limit, two series appear: low-energy expansion for low-lying meson states, and semiclassical expansion for highly excited states. The resulting series derived in [9, 13] contain corrections to the expressions (2.2) and (2.7).

The technique used in the analysis is presented in the next section on the example of the 't Hooft model.

2.2 't Hooft model

The 't Hooft model, or two-dimensional QCD with gauge group $SU(N)$, is defined by the following Lagrangian

$$\mathcal{L} = -\frac{N}{4g^2}\ \mathrm{Tr}\ F_{\mu\nu}F^{\mu\nu} + \bar{\psi}^{(a)}(i\gamma^\mu D_\mu - m_0^{(a)})\psi^{(a)}, \tag{2.23}$$

here $\psi^{(a)}$ are quarks with bare masses $m_0^{(a)}$, different in general; the field strength $F_{\mu\nu} = \partial_\mu A_\nu - \partial_\nu A_\mu + i\,[A_\mu,\ A_\nu]$ and the covariant derivative $D_\mu = \partial_\mu + iA_\mu$ are defined in terms of the gauge potential A_μ given by $N \times N$ hermitian traceless matrices. Being a two-dimensional gauge field theory, the model implies confinement via a linear potential, just like the IFT. Hence the qualitative interpretation of the particle spectrum together with the first terms in the asymptotic expansion of their masses, present in the IFT, is applicable to the 't Hooft model as well[5].

[5]The Hamiltonian, analogous to (2.1), has the same form with $2\bar{\sigma}h$, "the string tension" in the IFT, replaced by $g^2/2$.

In the large-N limit, 't Hooft derived the Bethe-Salpeter equation for mesons, two-quark bound states of the theory [26]. As it has already been pointed out, unlike in the IFT, this equation is exact when the number of colors is infinite. When quarks have equal masses $m_0^{(a)} = m_0$, which is the case we will consider, the 't Hooft equation has the form[6]

$$M^2\varphi(x) = \frac{m^2\,\varphi(x)}{x(1-x)} - \frac{g^2}{\pi}\int_0^1 \frac{\varphi(y)\;dy}{(y-x)^2} \tag{2.24}$$

with $\varphi(x)$ being the wave function of the meson with the mass M and $m^2 = m_0^2 - g^2/\pi$ standing for the renormalized quark mass, x and y are appropriately defined ratios of momenta of constituent quarks to the momentum of the meson. It is this equation (2.24) that is the main object of our analysis. Written in terms of dimensionless quantities, $\alpha = M^2/(4m^2)$ and $\lambda = g^2/(2m^2)$, the equation (2.24) becomes

$$\alpha\,\varphi(x) = \frac{\varphi(x)}{4x(1-x)} - \lambda\int_0^1 \frac{\varphi(y)}{(y-x)^2}\frac{dy}{2\pi}. \tag{2.25}$$

Again just like in the case of the IFT, the linear potential is hidden in the second term on the right hand side of the equation and is due to the presence of a double pole in the integrand.

The bound-state equation can be viewed as an eigenvalue problem $\hat{H}\varphi = \alpha\varphi$ for a suitably defined hamiltonian $\hat{H}$ acting in a certain Hilbert space. Solutions of the problem can be classified according to the symmetry $x \to 1-x$ of the equation giving rise to the odd and even solutions[7].

The overall goal of this work is to provide some insight into analytical properties of the spectrum, that is, properties of α as a function of λ taken complex. As we have pointed out earlier, at the current stage we will be mainly interested in asymptotic properties of the spectrum, analogous to the ones found for the IFT, leaving other, more interesting, questions for later.

---

[6]The derivation of the equation can be found, besides the original paper by 't Hooft [26], for example, in lectures by Coleman [33].

[7]In the IFT where there is just one type of fermions, the even sector is absent altogether.

2.2.1 Weak-coupling expansion

In the weak-coupling limit $\lambda \to 0$, each meson's mass M_n will approach $2m$ from above, i.e., α approaches 1_{+0}. Depending on how λ goes to 0, one gets different expansions. For example, if n is kept fixed, this limit will give us the low-energy expansion. This expansion appears to be in $t = \lambda^{1/3}$. At the same time if one looks at higher levels, with $n \geqslant 1/\lambda$, one obtains the semiclassical expansion that gives corrections to the already known Bohr–Sommerfeld quantization condition for the spectrum.

It is convenient to go to the rapidity space, $\theta = \frac{1}{2}\log\frac{x}{1-x}$. Then (2.25) takes the form[8]

$$\left(1 - \frac{\alpha}{\cosh^2\theta}\right)\varphi(\theta) = 2\lambda \fint_{-\infty}^{\infty} \frac{d\theta'}{2\pi} \frac{\varphi(\theta')}{\sinh^2(\theta-\theta')}. \tag{2.26}$$

Define the hamiltonian $\hat{H}$ as

$$\hat{H}\varphi(\theta) = \cosh^2\theta \left(\varphi(\theta) - 2\lambda \fint_{-\infty}^{\infty} \frac{d\theta'}{2\pi} \frac{\varphi(\theta')}{\sinh^2(\theta-\theta')}\right), \tag{2.27}$$

then (2.26) becomes equivalent to

$$\hat{H}\varphi(\theta) = \alpha\varphi(\theta) \tag{2.28}$$

with $\varphi(\theta)$ belonging to the Hilbert space with the metric identical to (2.22)

$$\|\varphi\|^2 = \int_{-\infty}^{\infty} \frac{d\theta}{2\pi} \frac{|\varphi(\theta)|^2}{4\cosh^2\theta}. \tag{2.29}$$

For $\varphi(\theta)$ we use the following ansatz

$$\varphi^{(0)}_{odd}(\theta) = \int_{-\infty}^{\infty} \frac{\sinh\theta\cosh\beta\ e^{iS(\beta)/\lambda}\ d\beta}{\sinh(\theta+\beta-i0)\sinh(\theta-\beta+i0)} \tag{2.30}$$

in the odd sector, and

$$\varphi^{(0)}_{even}(\theta) = \int_{-\infty}^{\infty} \frac{(-\sinh\beta\cosh\theta)\ e^{iS(\beta)/\lambda}\ d\beta}{\sinh(\theta+\beta-i0)\sinh(\theta-\beta+i0)} \tag{2.31}$$

in the even sector, where

$$S(\beta) = \alpha\tanh\beta - \beta. \tag{2.32}$$

[8] A quick look at this equation and the Bethe-Salpeter equation in the IFT (2.18) explains why we called the 't Hooft model rather simpler as a model in comparison with the IFT.

Both ansatz functions can be shown to be normalizable with respect to the metric (2.29).

In the further analysis we will be working with the following quantities

$$\sinh\theta\ \Delta_{odd}(\theta) \equiv (\hat{H}-\alpha)\varphi^{(0)}_{odd}(\theta) \tag{2.33}$$

and

$$-\cosh\theta\ \Delta_{even}(\theta) \equiv (\hat{H}-\alpha)\varphi^{(0)}_{even}(\theta). \tag{2.34}$$

Computation along the lines of the one shown in [13], sketched in the Appendix A, gives the following expressions for these functions

$$\Delta_{odd}(\theta) = \int_{-\infty}^{\infty} d\beta\ e^{iS(\beta)/\lambda}\left(\frac{\alpha}{\cosh\beta} - \frac{i\lambda\cosh^2\theta\sinh\beta}{(\cosh\beta+\cosh\theta)^2}\right), \tag{2.35}$$

$$\Delta_{even}(\theta) = \int_{-\infty}^{\infty} d\beta\ e^{iS(\beta)/\lambda}\left(\frac{\alpha\ \sinh\beta}{\cosh^2\beta} - \frac{i\lambda\cosh\theta\ (\cosh\beta\cosh\theta+1)}{(\cosh\beta+\cosh\theta)^2}\right). \tag{2.36}$$

We develop the small-λ series for (2.35) and (2.36). At first few orders, terms in these expansions will have no dependence on θ, directly giving the spectra α_n as zeroes of $\Delta_{odd/even}(\theta) \equiv \Delta_{odd/even}(\theta|\alpha)$. But in general, these terms will carry an explicit dependence on θ. In such situations one has to proceed as follows. Let $\{\varphi_n\}$ be the complete orthonormal set of eigenvectors of $\hat{H}$: $\hat{H}\varphi_n = \alpha_n\varphi_n$. Then the following quantity, set to zero,

$$C_{n;\,odd/even}(\alpha) = \left(\varphi_n, (\hat{H}-\alpha)\varphi^{(0)}_{odd/even}\right) \tag{2.37}$$

will play the role of the spectral condition with α_n being its zeroes. For small values of λ, $\varphi^{(0)}_{odd/even}$ provides a good approximation for φ_n. As λ grows, corrections can be found by iterating the following expression

$$\varphi_n(\theta) = \frac{1}{(\varphi_n, \varphi^{(0)}_{odd/even})}\left(\varphi^{(0)}_{odd/even}(\theta) - \sum_{k\neq n}\frac{C_k(\alpha)}{\alpha_k-\alpha}\varphi_k(\theta)\right). \tag{2.38}$$

Finding φ_n order by order and plugging it in (2.37), one obtains corrections to the spectral condition.

2.2.2 Low-energy expansion

Consider the case when α is close to 1, i.e., $M^2 \sim 4m^2$. Then we look for α in the form of a series in t

$$\alpha = 1 + zt^2 + \sum_{k=3}^{\infty} e_k t^k, \tag{2.39}$$

where z and e_k are to be determined. In this case one sees that the main contribution to the integrals (2.35) and (2.36) comes when $\beta \sim t$. Rescaling $\beta = -ut$, $\theta = -vt$, and observing that

$$\frac{S(\beta)}{\lambda} = S_0(u) + S_1(u), \tag{2.40}$$

where $S_0(u) = \frac{u^3}{3} - zu$ [9], and $S_1(u) = \frac{S(\beta)}{\lambda} - S_0(u) = O(t)$, one can expand $\Delta(\theta)$ in t. Subsequent setting terms in each order of t equal to zero gives conditions sufficient for determining α.

After a straightforward computation[10] one obtains low-energy expansions for α in both sectors. In the odd sector the first terms will have the form

$$\alpha_{odd} = 1 + t^2 z + \frac{t^4 z^2}{5} + t^6 \left(-\frac{3}{175} z^3 + \frac{6}{35} \right) + t^8 \left(\frac{23}{7875} z^4 - \frac{4}{1575} z \right) + \dots, \tag{2.41}$$

where z is any zero of the Airy function

$$\mathrm{Ai}(-z) = 0. \tag{2.42}$$

For even solutions one obtains

$$\alpha_{even} = 1 + t^2 z + t^4 \left(\frac{z^2}{5} + \frac{1}{5z} \right) + t^6 \left(-\frac{3}{175} z^3 + \frac{3}{25} - \frac{1}{50 z^3} \right) + \dots \tag{2.43}$$

with z being the solution of

$$\mathrm{Ai}'(-z) = 0. \tag{2.44}$$

---

[9] This part, $S_0(u)$, gives rise to the Airy function, which is an expected result due to the presence of the linear interaction.

[10] The calculation involves the integrals

$$\int_{-\infty}^{\infty} (iu)^k e^{iu^3/3 - izu} = \pi \mathrm{Ai}'(-z) I_k, \quad \int_{-\infty}^{\infty} (iu)^k e^{iu^3/3 - izu} = \pi \mathrm{Ai}(-z) J_k.$$

Both factors I_k and J_k satisfy the recursion relation

$$I_{k+2} = -z I_k + k I_{k-1}$$

with first of them following from (2.42) and (2.44), $I_0 = 0$, $I_1 = 1$, and $J_0 = 1$, $J_1 = 0$.

Looking at the terms in both series (2.41) and (2.43), one can identify them with successive approximations to the meson masses as follows: the t^0-term describes the bound state as two non-interacting quarks put together, the next term, $\sim t^2$, describes the correction due to the quark interaction via linear potential, the t^4-term is the leading relativistic correction. Higher order terms represent further relativistic corrections and corrections due to the short-range interaction between quarks.

As above, one should mention that except for the first few terms of the expansion of Δ in t, expressions at powers of t will depend on v, that is, on θ. In these cases one has to follow the procedure outlined above. We just note that such dependence appears for the first time at t^8-order in the odd sector and t^6-order in the even.

Looking at the coefficients in (2.41) and (2.43), one can see the general structure of e_k, polynomial in z or in z and $1/z$, respectively. At higher levels, z_n grow with n as $\sim n^{2/3}$ both for odd and even solutions. Hence, the leading terms in e_k, terms with the largest power of z, which come from the term at λ^0 in the brackets in (2.35) and (2.36), depend on the combination $(n^{1/3}t)^{2m}$. Moreover, one can notice that numerical coefficients are the same for both odd and even sectors. This is expected because the sum of these leading terms is given by the Bohr–Sommerfeld formula, the leading contribution in the semiclassical expansion. Therefore, one would expect that summing sub-leading terms should reproduce contributions of the semiclassical expansion of higher orders.

2.2.3 Semiclassics

When λ goes to zero and α is not necessarily close to 1, one obtains the semiclassical approximation. Technically it is reduced to calculating the integrals (2.35) and (2.36) using the saddle-point method.

In both sectors the integral for $\Delta(\theta)$ has the form

$$\Delta(\theta) = \int_{-\infty}^{\infty} d\beta\, f(\beta|\theta)\, e^{iS(\beta)/\lambda}, \tag{2.45}$$

where $f(\beta|\theta)$ is a linear function of λ. There are two saddle points $\beta = \pm\vartheta$ with ϑ being the positive solution of

$$\alpha = \cosh^2\vartheta. \tag{2.46}$$

Denoting contributions from $\pm\vartheta$ as $\Delta_\pm(\theta)$, we rewrite the integral as

$$\Delta(\theta) = \Delta_+(\theta) + \Delta_-(\theta). \tag{2.47}$$

In each case, odd or even, one has to compute only $\Delta_+(\theta)$, with $\Delta_-(\theta)$ coming from $\Delta_-(\theta) = \pm\Delta_+^*(\theta)$, here $+/-$ is in the odd and even sectors, respectively.

The leading order calculation yields the following expressions in the odd sector

$$\frac{\Delta_{odd}(\theta)\sqrt{\sinh\vartheta}}{2\sqrt{\pi\lambda\cosh^3\vartheta}} = \cos\left(\bar{S}(\vartheta)/\lambda - \pi/4\right), \tag{2.48}$$

and in the even

$$\frac{\Delta_{even}(\theta)}{2i\sqrt{\pi\lambda\sinh\vartheta\cosh\vartheta}} = \sin\left(\bar{S}(\vartheta)/\lambda - \pi/4\right) \tag{2.49}$$

with

$$\bar{S}(\vartheta) = S(\beta)|_{\beta=\vartheta} = \frac{\sinh 2\vartheta - 2\vartheta}{2}. \tag{2.50}$$

At this level, there is no dependence on θ, and the spectral condition in the leading order will have the Bohr–Sommerfeld form, $\bar{S}(\vartheta_n) = \pi\lambda(n - n_0)$, here $n = 1, 2, \ldots$, and n_0 is equal either to $1/4$ in the odd sector or $3/4$ in the even, just like in the qualitative analysis for the IFT above with the only difference due to the presence of the even solutions.

In contrast to the IFT, θ-dependence becomes relevant already at the one-loop level. Computations at this order give the following expression for the odd case

$$\frac{\Delta_{odd}(\theta)\sqrt{\sinh\vartheta}}{2\sqrt{\pi\lambda}\cosh^2\vartheta} = \cos\left(\bar{S}(\vartheta)/\lambda - \pi/4 + \lambda A_{odd}(\theta|\vartheta) + \lambda S_{1;\,odd}(\vartheta)\right), \tag{2.51}$$

where

$$A_{odd}(\theta|\vartheta) = -\frac{\cosh^2\theta\tanh\vartheta}{(\cosh\theta + \cosh\vartheta)^2}, \tag{2.52}$$

$$S_{1;\,odd}(\vartheta) = \frac{\tanh\vartheta}{4} + \frac{1}{48\tanh^3\vartheta}\left(-9\tanh^4\vartheta + 6\tanh^2\vartheta - 5\right). \tag{2.53}$$

In the even sector the expression is

$$\frac{\Delta_{even}(\theta)}{2i\sqrt{\pi\lambda\sinh\vartheta\cosh\theta}} = \sin\left(\bar{S}(\vartheta)/\lambda - \pi/4 + \lambda A_{even}(\theta|\vartheta) + \lambda S_{1;\,even}(\vartheta)\right) \tag{2.54}$$

with

$$A_{even}(\theta|\vartheta) = -\frac{\cosh\theta\,(\cosh\theta\cosh\vartheta + 1)}{\sinh\vartheta\,(\cosh\theta + \cosh\vartheta)^2}, \tag{2.55}$$

$$S_{1;\,even}(\vartheta) = \frac{1}{4\tanh^3\vartheta} + \frac{1}{48\tanh^3\vartheta}\left(-9\tanh^4\vartheta + 6\tanh^2\vartheta - 5\right). \tag{2.56}$$

In this situation one again has to use the method based on (2.37). At this order, when φ_n is approximated by $\varphi^{(0)}_{odd/even}$, the integral in (2.37) at small λ will have the main contribution coming from the saddle points $\theta = \pm\vartheta$ giving the following quantization conditions in the odd sector

$$\frac{\sinh 2\vartheta_n - 2\vartheta_n}{2} = \pi\lambda(n - 1/4) - \lambda^2\left(A_{odd}(\vartheta_n|\vartheta_n) + S_{1;\,odd}(\vartheta_n)\right) + O(\lambda^3) \tag{2.57}$$

and in the even sector

$$\frac{\sinh 2\vartheta_n - 2\vartheta_n}{2} = \pi\lambda(n - 3/4) - \lambda^2\left(A_{even}(\vartheta_n|\vartheta_n) + S_{1;\,even}(\vartheta_n)\right) + O(\lambda^3). \tag{2.58}$$

Once ϑ_n is found, the eigenvalues α_n are determined using (2.46).

Calculation in higher orders is technically similar, albeit more involved.

One can show that expansions (2.57) and (2.58) after a suitable change of variables reproduce results obtained in [35].

In principle, using (2.57) and (2.58) one can re-derive low-energy expansions (2.41) and (2.43), respectively.

2.2.4 Numerical results

Over the years there have been proposed different approaches to the numerical solution of the problem, each giving solution to 't Hooft's equation with any degree of accuracy. In [13] another method, based on discretizing the Fourier-transformed version of 't Hooft's equation, was suggested. Applying the Fourier transform to (2.26)

$$\varphi(\theta) = \int_{-\infty}^{\infty} d\nu\; e^{-i\nu\theta}\varphi(\nu), \quad \varphi(\nu) = \int_{-\infty}^{\infty} \frac{d\theta}{2\pi}\; e^{i\nu\theta}\,\varphi(\theta), \tag{2.59}$$

one obtains

$$\left(1 + \lambda\nu\coth\frac{\pi\nu}{2}\right)\varphi(\nu) = \alpha\int_{-\infty}^{\infty} d\nu'\; K(\nu - \nu')\varphi(\nu') \tag{2.60}$$

with $K(\nu) = \nu/(2\sinh\frac{\pi\nu}{2})$. The main feature of this version of 't Hooft's equation is the smoothness of its kernel allowing to discretize the equation directly. Even though this method can be not as efficient as others, its relative ease makes up for it. One

should mention that this is not the first time this parametrization involving Fourier transformed rapidity has been used. It has already appeared, for example, in [34] and recently in [35].

In Tables 2.1 and 2.2 we list values for α, i.e., for M^2 in units of $4m^2$, for first few levels, both odd and even, at different values of λ. Numerical results are obtained by discretizing (2.60) with the number of steps $N = 3000$ and step size $\varepsilon = 0.1$. This choice of discretization parameters provides more than sufficient accuracy in this range of λ, at least for the first levels. They are compared to the results obtained by means of derived expansions (2.41) and (2.43), truncated at $\lambda^{10/3}$ in the odd sector and at $\lambda^{8/3}$ in the even sector. One can see that within the given accuracy numerical results match the expected values with deviations determined by the order of the terms dropped from the low-energy expansion.

Table 2.1: α_n for first odd levels. The first value is numerical; the second is obtained using the truncated low-energy expansion (2.41); the third value is the order of the difference between the two.

λ	0.0001	0.001	0.01	0.1
$n = 1$	1.00504237411651 1.00504237411666 10^{-13}	1.02349036201 1.02349036216 10^{-10}	1.11087634 1.11087649 10^{-7}	1.55404 1.55418 10^{-4}
$n = 2$	1.00882272353899 1.00882272353917 10^{-13}	1.04121272921 1.04121272942 10^{-10}	1.19684999 1.19685027 10^{-7}	2.02721 2.02759 10^{-4}
$n = 3$	1.01192195048315 1.01192195048344 10^{-13}	1.05581244361 1.05581244407 10^{-10}	1.26911411 1.26911489 10^{-6}	2.44971 2.45097 10^{-4}
$n = 4$	1.01466422536562 1.01466422536618 10^{-12}	1.06878314251 1.06878314354 10^{-9}	1.33436550 1.33436743 10^{-6}	2.84797 2.85117 10^{-3}
$n = 5$	1.01717361844767 1.01717361844723 10^{-13}	1.08069521197 1.08069521405 10^{-9}	1.39513452 1.39513856 10^{-6}	3.23152 3.23815 10^{-2}

It is worthwhile to see the rate with which the expansions (2.41) and (2.43) approach the numerical values. For the lowest odd and even levels, which we choose because zeroes of $\mathrm{Ai}(-z)$ and $\mathrm{Ai}'(-z)$ are smallest for them thus making specific features of the expansions, especially in the even case, more prominent, this can be observed in Tables

Table 2.2: Same as in Table 2.1, but for first even levels.

λ	0.0001	0.001	0.01	0.1
$n=1$	1.002196798442 1.002196798481 10^{-11}	1.0102283943 1.0102284025 10^{-8}	1.0481649 1.0481666 10^{-6}	1.2387 1.2391 10^{-4}
$n=2$	1.007008105144 1.007008105149 10^{-12}	1.0326986818 1.0326986807 10^{-9}	1.1554011 1.1554000 10^{-6}	1.7964 1.7959 10^{-3}
$n=3$	1.010406331508 1.010406331481 10^{-11}	1.0486680231 1.0486680086 10^{-8}	1.2336564 1.2336495 10^{-5}	2.2408 2.2381 10^{-3}
$n=4$	1.013313818353 1.013313818267 10^{-10}	1.0623921932 1.0623921521 10^{-8}	1.3021422 1.3021238 10^{-5}	2.6502 2.6430 10^{-2}
$n=5$	1.015933386177 1.015933385994 10^{-10}	1.0748048015 1.0748047167 10^{-7}	1.3650255 1.3649880 10^{-5}	3.0406 3.0266 10^{-2}

2.3 and 2.4, respectively. Here $\alpha^{(k)}_{odd/even}$ denotes estimates obtained using (2.41) and (2.43) by keeping terms up to t^k included.

Table 2.3: Step-by-step approximation of the meson mass for the the lowest odd level obtained by successively including higher terms in (2.41); the last value is the numerical result.

λ	0.0001	0.001	0.01	0.1
$\alpha^{(2)}_{odd}$	1.00503729971412	1.02338107410	1.10852533	1.50373
$\alpha^{(4)}_{odd}$	1.00504237459180	1.02349040903	1.11088088	1.55448
$\alpha^{(6)}_{odd}$	1.00504237411491	1.02349036134	1.11087611	1.55400
$\alpha^{(8)}_{odd}$	1.00504237411666	1.02349036215	1.11087649	1.55418
$\alpha^{(num)}_{odd}$	1.00504237411651	1.02349036201	1.11087634	1.55404

Tables 2.5 and 2.6 contain values of α_n obtained through semiclassical expansions, (2.57) and (2.58). As expected, with n increasing, semiclassical results approach values obtained through discretization.

Again, it is useful to see how semiclassical formulae (2.57) and (2.58) approach results of direct numerical evaluation as one includes more terms in the expansion. These data are provided in Tables 2.7 and 2.8.

Table 2.4: Same as in Table 2.3, but for the lowest even level.

λ	0.0001	0.001	0.01	0.1
$\alpha_{even}^{(2)}$	1.002194922920	1.010187930	1.0472882	1.21949
$\alpha_{even}^{(4)}$	1.002196797651	1.010228320	1.0481584	1.23824
$\alpha_{even}^{(6)}$	1.002196798481	1.010228403	1.0481666	1.23907
$\alpha_{even}^{(num)}$	1.002196798442	1.010228394	1.0481649	1.23870

Table 2.5: α_n for first odd levels using semiclassics.

λ	0.0001	0.001	0.01	0.1
$n=1$	1.005045002	1.023502645	1.110935189	1.554453706
$n=2$	1.008822931	1.041213704	1.196854870	2.027350588
$n=3$	1.011921999	1.055812673	1.269115381	2.449829823
$n=4$	1.014664243	1.068783226	1.334366056	2.848080751
$n=5$	1.017173627	1.080695251	1.395134852	3.231630623

2.3 Discussion

The study of the mass spectrum in the low-temperature IFT and 't Hooft model presented here has to be considered as a part of an extended project. Further development of methods used in this work might provide a way to tackle more general problems. For example, as one of the possible extensions of the presented technique one can consider its application to the treatment of the 't Hooft model with arbitrary quark masses.

Not long ago another approach to the problem of the mass spectrum in the 't Hooft model was suggested in [35]. It is based on the fact that the bound-state equation can be reformulated as a certain difference equation. The method is rather general and can be applied to the IFT, as well as the 't Hooft model. To be more specific, under particular conditions on the analyticity of the solutions, one rewrites bound-state equations in both theories, (2.18) and (2.26)[11], in a homologous form as

$$Q(\nu+2i)+Q(\nu-2i)-2Q(\nu)=-\frac{4\alpha}{f(\nu)}\,Q(\nu). \tag{2.61}$$

The difference between the two theories lies solely in what $Q(\nu)$ and $f(\nu)$ are. Thus,

[11]It is convenient for this purpose first to rewrite them via the Fourier transform (2.59).

Table 2.6: α_n for first even levels using semiclassics.

λ	0.0001	0.001	0.01	0.1
$n=1$	1.002079962	1.009690485	1.045761963	1.229713753
$n=2$	1.007007280	1.032694849	1.155383793	1.796538843
$n=3$	1.010406206	1.048667441	1.233654091	2.240958482
$n=4$	1.013313781	1.062392019	1.302141769	2.650298641
$n=5$	1.015933371	1.074804730	1.365025460	3.040735165

Table 2.7: α_n for first odd levels from semiclassics; the first value is computed through the Bohr–Sommerfeld approximation; the second value includes the λ^2–correction; the third value is the numerical result.

λ	0.0001	0.001	0.01	0.1
$n=1$	1.005003824	1.023309966	1.109995180	1.547883056
	1.005045002	1.023502645	1.110935189	1.554453706
	1.005042374	1.023490362	1.110876342	1.554039023
$n=2$	1.008809448	1.041150166	1.196526952	2.023884388
	1.008822931	1.041213704	1.196854870	2.027350588
	1.008822724	1.041212729	1.196849986	2.027209388
$n=3$	1.011914598	1.055777568	1.268923891	2.447092290
	1.011921999	1.055812673	1.269115381	2.449829823
	1.011921950	1.055812444	1.269114113	2.449709791
$n=4$	1.014659340	1.068759829	1.334231284	2.845657897
	1.014664243	1.068783226	1.334366056	2.848080751
	1.014664225	1.068783143	1.334365504	2.847966326
$n=5$	1.017170044	1.080678054	1.395030374	3.229381199
	1.017173627	1.080695251	1.395134852	3.231630623
	1.017173618	1.080695212	1.395134525	3.231518812

in the IFT we set[12]

$$f(\nu) = 1 + \lambda\nu \tanh\frac{\pi\nu}{2}, \quad Q(\nu) = \cosh\frac{\pi\nu}{2}\, f(\nu)\,\varphi(\nu), \tag{2.62}$$

and in the 't Hooft model[13]

$$f(\nu) = 1 + \lambda\nu \coth\frac{\pi\nu}{2}, \quad Q(\nu) = \sinh\frac{\pi\nu}{2}\, f(\nu)\,\varphi(\nu). \tag{2.63}$$

Among the advantages of this approach one can name the most obvious one: it gives a hint at the presence of a certain integrable structure in both theories, since the the

[12]Here, in the IFT, α is defined in the same way as in the 't Hooft model, $\alpha = M^2/(4m^2)$.

[13]In [35], the authors consider the special case when the renormalized quark mass is zero.

Table 2.8: Same as in Table 2.7, but for the even levels.

λ	0.0001	0.001	0.01	0.1
$n=1$	1.002404341	1.011179464	1.052308851	1.251640571
	1.002079962	1.009690485	1.045761963	1.229713753
	1.002196798	1.010228394	1.048164905	1.238695902
$n=2$	1.007036829	1.032828428	1.155917112	1.796124444
	1.007007280	1.032694849	1.155383793	1.796538843
	1.007008105	1.032698682	1.155401066	1.796434578
$n=3$	1.010419587	1.048727116	1.233868841	2.239567100
	1.010406206	1.048667441	1.233654091	2.240958482
	1.010406332	1.048668023	1.233656383	2.240819014
$n=4$	1.013321943	1.062427975	1.302257261	2.648662328
	1.013313781	1.062392019	1.302141769	2.650298641
	1.013313818	1.062392193	1.302142228	2.650165065
$n=5$	1.015939061	1.074829509	1.365095410	3.039010202
	1.015933371	1.074804730	1.365025460	3.040735165
	1.015933386	1.074804802	1.365025482	3.040607676

difference equation above strongly reminds of the equation on Baxter's Q-operator which by itself indicates the integrability.

The overall project involving the IFT and 't Hooft model has many possible ramifications. Some of them are related to questions about analytical properties of the spectra which are preserved if one considers the case of number of colors large but finite in case of the 't Hooft model. In such cases one is primarily interested in the nature of singularities. Others deal with possible applications of these methods to more general field theories, theories with vacuum degeneracy, possessing certain integrabilty broken by perturbations. These perturbations typically give rise to a confining force between particles of original theories, just like in the case of the IFT and t' Hooft model which provide sufficiently simple examples of such theories.

Chapter 3

Scattering in high-temperature Ising field theory

In this chapter we concentrate our attention on the high-temperature limit of the IFT. In terms of the scaling variable η, this limit corresponds to $\eta \to -\infty$. As it has been argued earlier, at η sufficiently large the IFT can be viewed as a particle field theory with particles of one kind. Our primary interest is the high-energy scattering in this theory.

We approach the problem in a most natural way, via perturbation theory around the integrable point $\eta = -\infty$. We study the $2 \to 2$ scattering amplitude in the high-T domain using perturbation theory in h^2 to the leading order in h^2 [1]. Unfortunately, in its present form, this perturbation theory, as it has been noted earlier, is not as simple and transparent as the Feynman diagram technique. It relies on the intermediate-state decomposition with the use of exact matrix elements, also known as "form-factors", of the field $\sigma(x)$ at $h = 0$ that have already appeared in the previous chapter. One of the technical difficulties in such "form-factor" perturbation theory is that separating disconnected contributions and the "external leg" mass corrections is not as straightforward as in the standard Feynman technique. We bypass these difficulties by using the optical theorem and associated dispersion relation, expressing the amplitude through the total inelastic cross-section σ_{tot}. This procedure involves the well-known ambiguity in analytic terms, which can be fixed once the high-energy asymptotic of the amplitude is known. To eliminate this ambiguity we calculate this asymptotic directly (again, to the order of h^2), using an approach based on the intermediate-state decomposition and techniques developed in [10].

[1] The expansion goes in h^2 instead of h because of the Z_2-symmetry with respect to the change of the magnetization sign present in the high-T phase.

This chapter has the following structure. First, we remind the basics of the $2 \to 2$ scattering. Then based on the intermediate-state decomposition and dispersion relation for the amplitude we compute the dominant contributions to the amplitude and the cross-section for this process. In the following section we use the known relation between the matrix element for the amplitude and the classical sinh-Gordon problem to compute the large-energy asymptotic of the amplitude. Finally, we present a semiclassical argument about the behavior of the amplitude of the process beyond the leading order.

3.1 General properties of $2 \to 2$ S-matrix element

In this section we briefly describe general properties of the $2 \to 2$ scattering matrix element and the $2 \to n$ inelastic cross-section. For the most part, the content of this section is an adaptation of textbook basics of the relativistic S-matrix theory (see, e.g., [37]), with minor simplifications specific for the $1+1$-kinematics.

For simplicity, and in view of the problem at hand, we assume that the theory has one neutral particle, with the mass m, which we refer to as the particle A. Kinematic state of the asymptotic particle is characterized by its on-shell 2-momentum p^μ, conveniently parametrized by the rapidity θ, $p(\theta) \equiv p^\mu(\theta) = (m\cosh\theta, m\sinh\theta)$. We use the notations

$$|\theta_1, \theta_2, \dots, \theta_n\rangle_{in(out)} \tag{3.1}$$

for the in- (out-) states with n particles A, with the rapidities θ_1, θ_2, …, θ_n. The states form the Fock space, and we assume the following normalization of one-particle states

$$\langle\theta|\theta'\rangle = (2\pi)\,\delta(\theta - \theta'). \tag{3.2}$$

In two dimensions, the $2 \to 2$ scattering is always purely elastic (i.e., the momenta of the two outgoing particles are the same as the momenta of the incoming ones), by the total energy-momentum conservation. Therefore, one can write

$$|\theta_1, \theta_2\rangle_{in} = S_{2\to2}(\theta_1, \theta_2)|\theta_1, \theta_2\rangle_{out} + \sum_{n=3}^{\infty} \frac{1}{n!} \int \prod_{i=1}^{n} \frac{d\beta_i}{2\pi} \times$$
$$\times\, (2\pi)^2 \delta^{(2)}(P_{in} - P_{out}) S_{2\to n}(\theta_1, \theta_2|\beta_1, \dots, \beta_n)|\beta_1, \dots, \beta_n\rangle_{out}, \tag{3.3}$$

where $P_{in} = p(\theta_1) + p(\theta_2)$ and $P_{out} = \sum_{i=1}^{n} p(\beta_i)$ are the total 2-momenta of the initial and the final states, respectively. The equation (3.3) defines the $2 \to n$ S-matrix elements $S_{2\to n}$. Our attention will be mostly focussed on the element $S_{2\to 2}(\theta_1, \theta_2)$. Relativistic invariance demands that it actually depends on a single variable, the rapidity difference $\theta_1 - \theta_2$; correspondingly, we will write

$$S_{2\to 2}(\theta_1, \theta_2) \equiv S(\theta_1 - \theta_2). \tag{3.4}$$

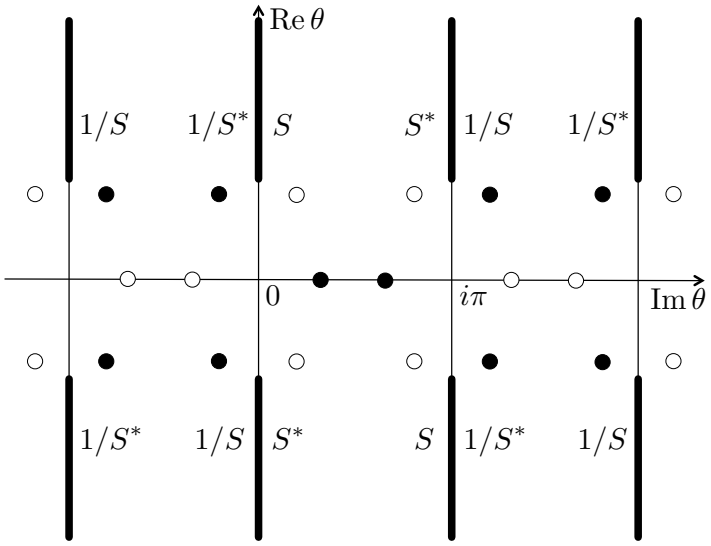

Figure 3.1: Analytic structure of the two-particle scattering amplitude $S(\theta)$ in the complex θ-plane. The thick lines represent the branch cuts associated with inelastic channels. The values of $S(\theta)$ at different edges of the cuts represent physical S-matrix element S, its complex conjugate S^*, and the inverse values. The bullets $\bullet$ and circles $\circ$ indicate possible positions of poles and zeroes, respectively. Poles located on the imaginary axis within the physical strip $0 < \mathrm{Im}\,\theta < \pi$ correspond to stable particles, poles in the mirror strip $-\pi < \mathrm{Im}\,\theta < 0$ are associated with resonance scattering states.

The function $S(\theta)$ has direct physical interpretation at real values of θ (the physical domain in the s-channel scattering), but it can be analytically continued to the complex θ-plane with certain singularities. The analyticity of $S(\theta)$ was widely discussed in the specific context of factorizable scattering theory (see, e.g., [6]), but much of this analysis is applicable in the general case. The function $S(\theta)$ is analytic in the strip $0 < \mathrm{Im}\,\theta < \pi$, except for possible poles at the corresponding segment of the imaginary-θ axis (such

poles, if present, signify stable particles existing in the theory). $S(\theta)$ takes real values at purely imaginary θ. The function admits analytic continuation to the whole θ-plane (with certain branch cuts, as is detailed below) via the functional relations

$$S(\theta) = S(i\pi - \theta), \tag{3.5}$$

$$S(\theta)S(-\theta) = 1. \tag{3.6}$$

The first of these relations expresses the crossing symmetry of the S-matrix. The second follows from the unitarity of the $2 \to 2$ S-matrix at the energies below the multi-particle thresholds. In the case of integrable, purely elastic scattering theory, the multi-particle contributions to (3.3) are altogether absent, and as the result in this case $S(\theta)$ is a meromorphic function of the whole complex plane. But in the general, non-integrable, case, of course, branching-point singularities associated with the multi-particle thresholds are present. These branching points are located at $\theta = \pm\theta^{(n)}$, where $\theta^{(n)}$ are real positive solutions of the equation

$$\cosh\frac{\theta^{(n)}}{2} = \frac{n}{2}, \tag{3.7}$$

and they correspond to the n-particle thresholds. By the crossing symmetry (3.5), there are similar branching points at the axis $\mathrm{Im}\,\theta = \pi$, $\theta = i\pi \mp \theta^{(n)}$ representing the n-particle thresholds in the cross-channel. Since the relations (3.5) and (3.6) imply periodicity

$$S(\theta + 2\pi i) = S(\theta), \tag{3.8}$$

the pattern is periodically extended along the imaginary-θ axis. We will define the principal sheet of the θ-surface by making branch cuts from $\theta^{(n)}$ to $+\infty$ and from $-\theta^{(n)}$ to $-\infty$, with periodic extension according to (3.8), as is shown in Fig. 3.1 (note the unusual directions of the axes in this figure). Presumably, $S(\theta)$ can be further analytically continued under the branch cuts, to other sheets of the Riemann surface, but at the moment we do not have much to say about its analytic structure there. Discontinuities of $S(\theta)$ across the branch cuts are controlled by the probabilities of inelastic scattering events. As follows from the full unitarity condition, we have, at real

positive θ,

$$S(\theta + i0)S(-\theta + i0) = S(\theta + i0)/S(\theta - i0) = 1 - \sigma_{tot}(\theta), \tag{3.9}$$

where $\sigma_{tot}(\theta)$ is the total probability of all inelastic processes,

$$\sigma_{tot}(\theta) = \sum_{n=3}^{\infty} \sigma_{2\to n}(\theta), \tag{3.10}$$

$$\sigma_{2\to n}(\theta) = \frac{1}{\sinh\theta}\frac{1}{n!}\left[\int \prod_{i=1}^{n} \frac{d\beta_i}{2\pi}\right](2\pi)^2\delta^{(2)}(P_{in} - P_{out})\,|S_{2\to n}(\theta_1,\theta_2|\beta_1,\ldots,\beta_n)|^2\,.$$

In the last line, the notations are the same as in (3.3). Obviously, $\sigma_{2\to n}(\theta) = 0$ at $|\theta| < \theta^{(n)}$, and hence the total cross-section (3.10) has the segment $[\theta^{(3)}, \infty)$ as its support.

Apart from these branch cuts, $S(\theta)$ can have poles at the principal sheet. Due to the periodicity (3.8), one can limit attention to the strip $-\pi \leqslant \mathrm{Im}\,\theta \leqslant \pi$. We will refer to the domain $0 < \mathrm{Im}\,\theta < \pi$ as the "physical strip" (PS), since the values of $S(\theta)$ at its boundaries represent physical scattering amplitudes. In view of (3.6), every pole of $S(\theta)$ in the PS is accompanied by the associated zero in the strip $-\pi < \mathrm{Im}\,\theta < 0$ and vice versa, and for this reason we refer to the latter as the "mirror strip" (MS). By causality, locations of possible poles within the PS are limited to the imaginary axis $\mathrm{Re}\,\theta = 0$. The poles in the PS are associated with stable particles of the theory. In a unitary theory, a pole at $\theta = i\alpha_p$ (with $0 < \alpha_p < \pi$),

$$S(\theta) \approx \frac{ir_p}{\theta - i\alpha_p}, \tag{3.11}$$

with positive r_p, is the direct-channel manifestation of the stable particle ("bound state") A_p with the mass $M_p = 2\cos(\alpha_p/2)$. Every such pole comes along with the cross-channel pole at $i\tilde{\alpha}_p \equiv i(\pi - \alpha_p)$, with the residue $-ir_p{}^2$. On the other hand, poles in the MS are not restricted to lie at the imaginary axis $\mathrm{Re}\,\theta = 0$. There may be poles at $i\alpha_p$ with real $\alpha_p \in [-\pi, 0]$ ("virtual states", in the terminology of the potential scattering theory), as well as with a complex α_p (generally associated with resonance states).

---

[2] Of course, strict adherence to our assumption that there is only one kind of stable particles implies that there can be only two poles in the PS, at $i\alpha_A = 2\pi i/3$ and at $i\tilde{\alpha}_A = i\pi/3$.

If the positions of all the poles on the principal sheet are known, the function $S(\theta)$ can be written as

$$S(\theta) = \prod_p \frac{\sinh\theta + i\sin\alpha_p}{\sinh\theta - i\sin\alpha_p}\, U(\theta), \tag{3.12}$$

where the product accounts for all the poles $\theta = i\alpha_p$, $i(\pi-\alpha_p)$, including bound, virtual, and resonance states. The function $U(\theta)$ satisfies the same relations (3.5) and (3.6), together with (3.9), as the amplitude $S(\theta)$, but in addition it has neither poles nor zeroes, on the whole principal sheet. Hence it can be written as

$$U(\theta) = \exp\left(i\sinh\theta\,\Delta(\theta)\right), \tag{3.13}$$

with $\Delta(\theta)$ analytic everywhere in the PS. As follows from (3.5) and (3.6), $\Delta(\theta)$ satisfies the relations

$$\Delta(\theta) = \Delta(i\pi - \theta), \quad \Delta(\theta) = \Delta(-\theta), \tag{3.14}$$

which in turn imply an enhanced periodicity

$$\Delta(\theta + i\pi) = \Delta(\theta). \tag{3.15}$$

Of course, $\Delta(\theta)$ has branching points at the thresholds $\theta^{(n)}$, and in view of (3.9), its discontinuities across the associated branch cuts are related to the inelastic cross-sections. In particular, at positive real θ we have

$$\Delta(\theta + i0) - \Delta(\theta - i0) = -\frac{i\log\left(1 - \sigma_{tot}(\theta)\right)}{\sinh\theta}. \tag{3.16}$$

In view of (3.14) and (3.15), it suffices to concentrate attention on the values of $\Delta(\theta)$ in the strip $0 \leqslant \mathrm{Im}\,\theta \leqslant \pi/2$. The transformation

$$w = \sinh^2\theta \tag{3.17}$$

maps this domain (with obvious identifications at the boundary) onto the complex w-plane with the branch cut along the real axis, from $w^{(3)} = \sinh^2\theta^{(3)} = 45/4$ to $+\infty$[3].

[3]It is useful to understand the mapping properties of (3.17). The edges $\mathrm{Im}\,\theta = +0$ of the branch cuts $\theta \in [\theta^{(3)}, +\infty)$ and $\theta \in (-\infty, -\theta^{(3)}]$ in Fig. 3.1 correspond to the upper and lower edges of the branch cut in the w-plane. The segment $[0, \theta^{(3)}]$ of the imaginary θ-axis is mapped onto the segment $[0, w^{(3)}]$ of the real w-axis. Furthermore, the segments $[-1, 0]$ and $(-\infty, -1]$ of the real w-axis are the images of the segments $\mathrm{Re}\,\theta = 0$, $\mathrm{Im}\,\theta \in [0, \pi/2]$ and $\mathrm{Im}\,\theta = \pi/2$, $\mathrm{Re}\,\theta \in [0, +\infty)$, respectively.

We note that w relates to the center-of-mass energy $E = 2m\cosh(\theta/2)$ as

$$w = \frac{E^2(E^2-4m^2)}{4m^2}. \tag{3.18}$$

With some abuse of notations, let us write $\Delta(w)$ and $\sigma_{tot}(w)$ for the quantities defined in (3.10) and (3.13), expressed in terms of the variable w. The equation (3.16) then relates the discontinuity of $\Delta(w)$ across the branch cut in the w-plane to $\sigma_{tot}(w)$, and one can write down the associated dispersion relation

$$\Delta(w) = \Delta_{reg}(w) + i\int_{w^{(3)}}^{\infty} \frac{\log\left(1-\sigma_{tot}(v)\right)}{(w-v)\sqrt{v}}\frac{dv}{2\pi}, \tag{3.19}$$

where $\Delta_{reg}(w)$ is an entire function of w, real at the real w-axis[4].

3.2 Scattering in IFT at weak coupling

Let us come back to the theory (1.4), and consider the particle scattering in the high-T regime, at weak coupling $|h| \ll \tau^{15/8}$. In this domain there is only one stable particle [4], which in the absence of the magnetic field, $h = 0$, becomes a free Majorana fermion. In this case the scattering is trivial and $S(\theta)|_{h=0} = -1$ [5]. At small h the amplitude $S(\theta)$ can be expressed as series in powers of h^2. Here we mostly limit our attention to the leading term of this expansion, the amplitude $A(\theta)$ defined as

$$S(\theta) = -\left(1 + h^2\,\frac{iA(\theta)}{\sinh\theta} + O(h^4)\right). \tag{3.20}$$

To simplify notations, in what follows we set the units of mass so that $m = 1$.

The amplitude $A(\theta)$ is analytic in the PS, except for the poles at $i\alpha_A = 2\pi i/3$ and $i\tilde{\alpha}_A = i\pi/3$, representing the particle A itself in the direct- and cross-channels, respectively. Note that in view of the overall minus sign in (3.20), the residue at $i\alpha_A$ must be negative. From (3.5) and (3.6) it follows that $A(\theta)$ satisfies the same symmetries

[4]The integral can diverge if σ_{tot} approaches its unitarity bound 1 at high energies too fast; as usual, in such cases one has to make appropriate subtractions.

[5]In 1 + 1-dimensions it is useful to distinguish between in- and out-states even in a free fermion theory. Thus, in the IFT with $h = 0$, the n-particle in-state with $\theta_1 > \theta_2 > \ldots > \theta_n$ is identified with the Fock-space state $|\theta_1, \ldots, \theta_n\rangle \equiv a^\dagger(\theta_1)\ldots a^\dagger(\theta_n)|0\rangle$, while for the out-state the fermion creation operators must be arranged in the opposite order.

as $\Delta(\theta)$ in (3.14), i.e.,

$$A(\theta) = A(i\pi - \theta), \qquad A(\theta) = A(-\theta), \tag{3.21}$$

and $A(\theta + i\pi) = A(\theta)$. We will see that

$$A(0) = 0. \tag{3.22}$$

Again, expressing $A(\theta)$ as a function of w, we conclude that this function is analytic in the whole w-plane, with the branch cut from $w^{(3)}$ to $+\infty$, except for a single pole at $w = -3/4$. The discontinuity of $A(w)$ across the branch cut is related to the cross-section

$$A(w + i0) - A(w - i0) = i\sqrt{w}\,\sigma^{(2)}_{tot}(w), \tag{3.23}$$

where $\sigma^{(2)}_{tot}$ is the leading term of the expansion

$$\sigma_{tot}(w) = h^2\sigma^{(2)}_{tot}(w) + O(h^4). \tag{3.24}$$

Assuming that $A(w) \sim \sqrt{w}\log w$ as $w \to \infty$, an assumption that we will verify later on, and making use of (3.22), based on (3.23) we can write down the corresponding dispersion relation

$$A(w) = \frac{rw}{w + 3/4} + w\int_{w^{(3)}}^{\infty} \frac{\sigma^{(2)}_{tot}(v)}{(v - w)\sqrt{v}}\frac{dv}{2\pi} \tag{3.25}$$

with r being a constant, yet to be determined.

Of course, the amplitude $A(\theta)$ admits standard perturbation theory representation in the form of the integral

$$iA(\theta_{12}) = -\frac{1}{2}\int d^2x\ \langle\theta_1, \theta_2|T\sigma(x)\sigma(0)|\theta_1, \theta_2\rangle_{conn}, \tag{3.26}$$

where the integration goes over Minkowski space-time, $x = (\mathrm{x}, \mathrm{t})$, and $\theta_{12} \equiv \theta_1 - \theta_2$. The integrand involves the connected part of the time-ordered product[6] of the Heisenberg

[6]The connected part is obtained from the full matrix element by removing its disconnected parts

$$\langle\theta_1, \theta_2|T\sigma(x)\sigma(0)|\theta_1', \theta_2'\rangle_{conn} = \langle\theta_1, \theta_2|T\sigma(x)\sigma(0)|\theta_1', \theta_2'\rangle - 2\pi\delta(\theta_1 - \theta_1')\langle\theta_2|T\sigma(x)\sigma(0)|\theta_2'\rangle - \\ - 2\pi\delta(\theta_2 - \theta_2')\langle\theta_1|T\sigma(x)\sigma(0)|\theta_1'\rangle - (2\pi)^2\delta(\theta_1 - \theta_1')\delta(\theta_2 - \theta_2')\langle 0|T\sigma(x)\sigma(0)|0\rangle \tag{3.27}$$

before setting $\theta_1' = \theta_1'$, $\theta_2' = \theta_2$. In writing (3.27) we have omitted the terms involving $\delta(\theta_1 - \theta_2')$ and $\delta(\theta_1' - \theta_2)$, which are generally present by the antisymmetry of the matrix element with respect to $\theta_1 \leftrightarrow \theta_2$, because they vanish at $\theta_1' = \theta_1'$, $\theta_2' = \theta_2$.

field operators. The matrix element in (3.26) can be handled through the intermediate-state decomposition with the use of the exact matrix elements from [27],

$$F(\theta_1,\theta_2|\beta_1,\dots,\beta_n) = \langle\theta_1,\theta_2|\sigma(0)|\beta_1,\dots,\beta_n\rangle = i^{(n+2)/2}\bar{\sigma}\tanh\left(\frac{\theta_1-\theta_2}{2}\right)\times \\ \times\prod_{i=1}^{n}\left[\coth\left(\frac{\theta_1-\beta_i}{2}\right)\coth\left(\frac{\theta_2-\beta_i}{2}\right)\right]\prod_{i<j}\tanh\left(\frac{\beta_i-\beta_j}{2}\right). \quad (3.28)$$

Since the form-factors (3.28) vanish at $\theta_1-\theta_2=0$, this expansion directly confirms (3.22). However, this approach has well-known difficulties. In particular, individual n-particle contributions are not Lorentz-invariant, this symmetry being restored only upon summing up all multi-particle terms. For this reason, it is easier to collect the multi-particle contributions by using the dispersion relation (3.25), expressing the amplitude through the h^2-term of the inelastic cross-section (3.24). The latter can be written in terms of the form-factors (3.28) as

$$\sigma^{(2)}_{tot}(w) = \sum_{k=1}^{\infty}\sigma^{(2)}_{2\to 2k+1}(w) \quad (3.29)$$

with

$$\sigma^{(2)}_{2\to n}(w) = \frac{1}{\sqrt{\omega}}\frac{1}{n!}\int\left[\prod_{i=1}^{n}\frac{d\beta_i}{2\pi}\right](2\pi)^2\delta^{(2)}\left(P_{in}-P_{out}\right)|F(\theta_1,\theta_2|\beta_1,\dots,\beta_n)|^2,$$

here $w=\sinh^2(\theta_1-\theta_2)\equiv\sinh^2\theta$. In writing (3.29), we take into account that matrix elements of $F(\theta_1,\theta_2|\beta_1,\dots,\beta_n)$ with even n vanish. This leaves undetermined the coefficient r in the pole term in (3.25), which should be evaluated separately.

3.2.1 Pole term

The residue of $A(\theta)$ at the pole $\theta=2\pi i/3$ can be deduced from the one-particle term in the standard intermediate-state decomposition (3.26),

$$A(\theta_{12}) = -\int_{-\infty}^{\infty}d\beta\ \frac{\delta(\sinh\theta_1+\sinh\theta_2-\sinh\beta)}{\cosh\theta_1+\cosh\theta_2-\cosh\beta+i0}|\langle\theta_1,\theta_2|\sigma(0)|\beta\rangle|^2+\dots, \quad (3.30)$$

where ... stands for the multi-particle contributions. With the use of explicit matrix elements (3.28), we have

$$|\langle\theta_1,\theta_2|\sigma(\theta)|\beta\rangle|^2 = \bar{\sigma}^2\tanh^2\left(\frac{\theta_1-\theta_2}{2}\right)\coth^2\left(\frac{\theta_1-\beta}{2}\right)\coth^2\left(\frac{\beta-\theta_2}{2}\right). \quad (3.31)$$

Since the expression is positive at all real values of the rapidities, we have erased the absolute value signs, making possible analytical continuation to the complex plane. The integral over β is eliminated by the delta-function[7], and the result explicitly shows a pole at $\theta \equiv \theta_1 - \theta_2 = 2\pi i/3$,

$$A(\theta) \approx -\frac{i18\sqrt{3}\,\bar{\sigma}^2}{\theta - 2\pi i/3}. \tag{3.32}$$

Note that the minus sign here appears because analytical continuation of the right-hand side of (3.31) to the pole point yields real but negative value

$$-\tanh^6(2\pi/3) = -27.$$

This, when combined with the overall minus sign in (3.20), (3.32) shows $2\pi i/3$ to be a positive pole of $S(\theta)$,

$$S(\theta) \approx \frac{i36(\bar{\sigma}h)^2}{\theta - 2\pi i/3} + O(h^4). \tag{3.33}$$

The cross-channel pole at $\theta = \pi i/3$, which will have a residue with the opposite sign, can be extracted from the three-particle contribution to the intermediate-state decomposition, which also generates the threshold singularity at $\theta^{(3)}$. The higher multi-particle terms do not contribute to the residues, producing only the associated multi-particle threshold singularities. The residue in (3.32) corresponds to the value

$$r = 36\bar{\sigma}^2 \tag{3.34}$$

of the coefficient in (3.25).

3.2.2 Three- and multi-particle contributions to $\sigma_{tot}^{(2)}$

The first term in (3.29), $\sigma_{2\to3}^{(2)}$, can be evaluated in closed form (see Appendix C for details). When expressed in terms of the center-of-mass energy

$$E = 2\cosh(\theta/2),$$

it can be written as

$$\sigma_{2\to3}^{(2)}(E) = \Theta(E-3)N(E)I(E), \tag{3.35}$$

[7]It is easiest to do this calculation in the center-of-mass frame $\theta_1 + \theta_2 = 0$. Although the one-particle term (3.30) is not Lorentz-invariant, the residue at the pole is.

where the step-function $\Theta(E-3)$ is put as a reminder that this part of the cross-section vanishes below the three-particle threshold,

$$N(E) = \frac{4\bar{\sigma}^2}{\pi}\frac{(E+2)^{5/2}}{(E-2)^{3/2}}\frac{(E-3)^3(2E-1)^4}{(E+3)^{3/2}(E-1)^{5/2}(E+1)E^3}, \tag{3.36}$$

and $I(E)$ is the elliptic integral of the form

$$I(E) = \int_{-1}^{1} dt\,\frac{\sqrt{1-t^2}}{(1-q\,t^2)^{3/2}}\left(\frac{1-\mu\,t^2}{1-\nu\,t^2}\right)^2 \tag{3.37}$$

with

$$q = \frac{(E+1)(E-3)^3}{(E-1)(E+3)^3}, \quad \mu = q\,\frac{(E-2)(2E+1)^2}{(E+2)(2E-1)^2}, \quad \nu = q\,\frac{E+2}{E-2}. \tag{3.38}$$

Some basic properties of $\sigma^{(2)}_{2\to3}(E)$ are readily derived. For example, near the threshold $E \to 3$ the leading term is

$$\sigma^{(2)}_{2\to3}(E) = \frac{5^6\sqrt{5}\,\bar{\sigma}^2}{2^5 3^4\sqrt{3}}\,\Theta(E-3)\,(E-3)^3 + O\left((E-3)^4\right). \tag{3.39}$$

On the other hand, at large E the behavior is given by

$$\sigma^{(2)}_{2\to3}(E) = \frac{32\bar{\sigma}^2}{\pi}\left(\log E^2 + \frac{\sqrt{3}\pi - 11}{2} + O\left(1/E^2\right)\right). \tag{3.40}$$

The behavior of $\sigma^{(2)}_{2\to3}(E)$ near the threshold and at large E and how well the asymptotic expressions (3.39) and (3.40) approximate the exact value are shown in Figs. 3.2 and 3.3, respectively.

Another useful conclusion can be made about the behavior of $\sigma^{(2)}_{2\to n}(E)$ at the n-particle threshold, $E \to n$. The computation, sketched in Appendix D, shows that $\sigma^{(2)}_{2\to n}(E)$ decays to zero according to

$$\sigma^{(2)}_{2\to n}(E) = \Theta(E-n)\,\frac{2\sqrt{n^2-4}}{n^3}\frac{\bar{\sigma}^2}{2^{n^2-n}}\times \\ \times\left(\frac{n+2}{n-2}\right)^{2n}\frac{\prod_{p=1}^{n-1}p!}{\sqrt{n}}\frac{(E-n)^{(n^2-3)/2}}{(2\pi)^{(n-3)/2}\,\Gamma\left(\frac{n^2-1}{2}\right)} + O\left((E-n)^4\right). \tag{3.41}$$

Except for the threshold asymptotics, the partial cross-sections $\sigma^{(2)}_{2\to n}$ with $n > 3$ are not evaluated in closed form. However, numerical estimates show that these multi-particle terms are small when compared to $\sigma^{(2)}_{2\to3}$ at all values of the energy E. Thus, the five-particle contribution $\sigma^{(2)}_{2\to5}$ is smaller than 1% of $\sigma^{(2)}_{2\to3}$ at all E, and the higher terms are small still. Therefore, the amplitude $A(\theta)$ in (3.20) can be approximated with high accuracy by the dispersion relation (3.25) with $\sigma^{(2)}_{tot}(w)$ replaced by $\sigma^{(2)}_{2\to3}(w)$.

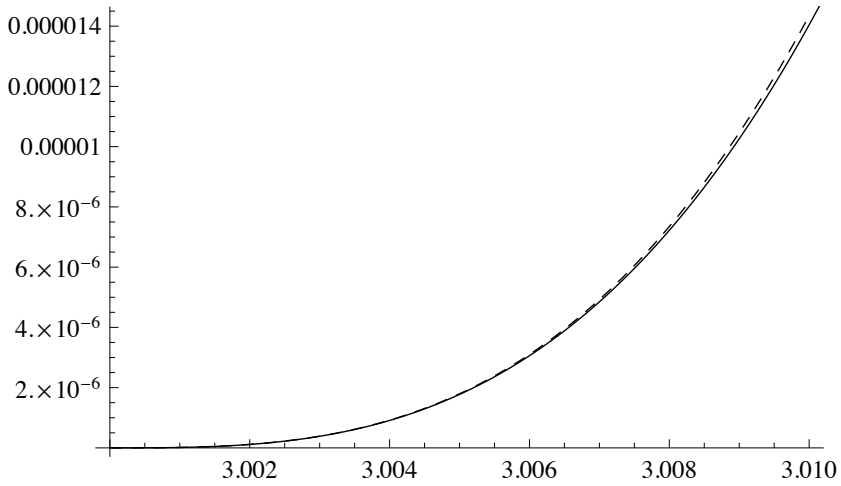

Figure 3.2: Threshold behavior of $\sigma^{(2)}_{2\to3}(E)$; the solid line is the result of the numerical evaluation of $\sigma^{(2)}_{2\to3}(E)$, the dashed line shows the asymptotic form (3.39).

3.2.3 The amplitude

With $\sigma^{(2)}_{tot}(w)$ approximated by $\sigma^{(2)}_{2\to3}(w)$, the second term in (3.25), which we denote as $A_\sigma(w)$, can be evaluated numerically. The relative contributions of $A_\sigma(w)$ and the pole term $A_p(w) = 36\bar\sigma^2 w/(w+3/4)$ in (3.25) for low values of w are shown in Fig. 3.4. One can see that in the shown domain of w the pole term brings substantially larger contribution than $A_\sigma(w)$. In particular, in the physical domain $w > 0$, but below the three-particle threshold $w^{(3)} = 11.25$, $A_\sigma(w)$ contributes no more than 15% to the scattering phase. Above the threshold, $w > w^{(3)}$, $A_\sigma(w)$ develops imaginary part, $\sqrt{w/4}\,\sigma^{(2)}_{2\to3}$. At larger w the real part of $A_\sigma(w)$ increases, overtaking at $w \approx 68.31$ the pole term $A_p(w)$ in magnitude, and then approaches the asymptotic $8\bar\sigma^2\sqrt{w}$. At large negative w, $A_\sigma(w)$ behaves as $-(8\bar\sigma^2/\pi)\sqrt{-w}\log(-w/w_0) - 36\bar\sigma^2$ with $w_0 = (1/4)\exp(11-\sqrt{3}\,\pi) \approx 64.86$. Figs. 3.5 and 3.6 show how the real and imaginary parts of $A_\sigma(w)$ are approximated by its large w-asymptotic $-(8\bar\sigma^2/\pi)\sqrt{-w}\log(-w/w_0) - 36\bar\sigma^2$.

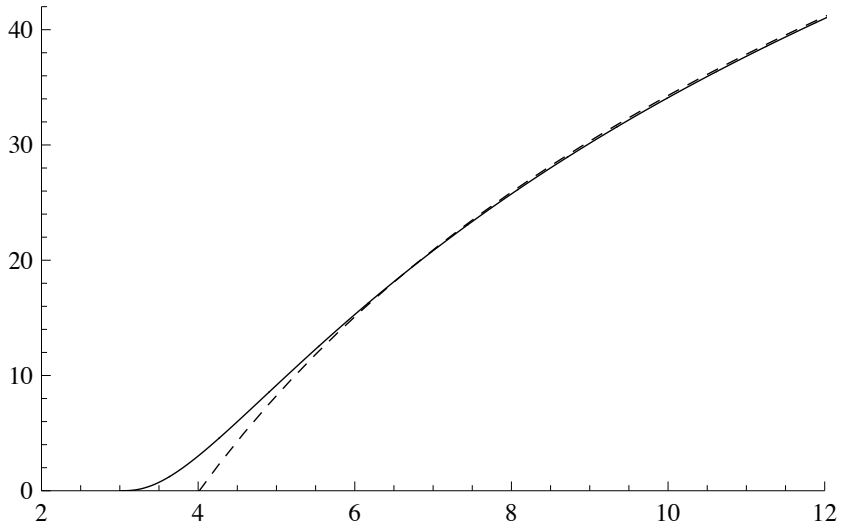

Figure 3.3: Large-E behavior of $\sigma^{(2)}_{2\to 3}(E)$; the solid line is the result of the numerical evaluation of $\sigma^{(2)}_{2\to 3}(E)$, the dashed line shows the asymptotic form (3.40), which is seen to approximate $\sigma^{(2)}_{2\to 3}(E)$ very closely starting from relatively low energies.

3.3 High-energy limit of the amplitude

In the IFT with $h = 0$, the matrix element in (3.26) admits the exact representation in terms of the Lax equation associated with special solution of the classical sinh-Gordon equation. In this section we describe this relation and then use it to evaluate the asymptotic of $A(\theta_{12})$ at high energy, $\theta_{12} \to \infty$.

3.3.1 The matrix element

As is known since the classic paper [38], the two-point correlation functions of the spin field σ and the disorder field μ in the $h = 0$ IFT, $G(x) = \langle 0|T\sigma(x)\sigma(0)|0\rangle$ and $\tilde{G}(x) = \langle 0|T\mu(x)\mu(0)|0\rangle$, are expressed in terms of a special solution of the classical sinh-Gordon system

$$\partial_{\mathrm{z}}\partial_{\bar{\mathrm{z}}}\varphi = \frac{1}{8}\sinh(2\varphi)\,, \quad \partial_{\mathrm{z}}\partial_{\bar{\mathrm{z}}}\chi = \frac{1}{8}\left[1-\cosh(2\varphi)\right]. \tag{3.42}$$

Here and below we use the light-cone coordinates z and $\bar{\mathrm{z}}$

$$\mathrm{z} = \mathrm{x} - \mathrm{t}, \quad \bar{\mathrm{z}} = \mathrm{x} + \mathrm{t} \tag{3.43}$$

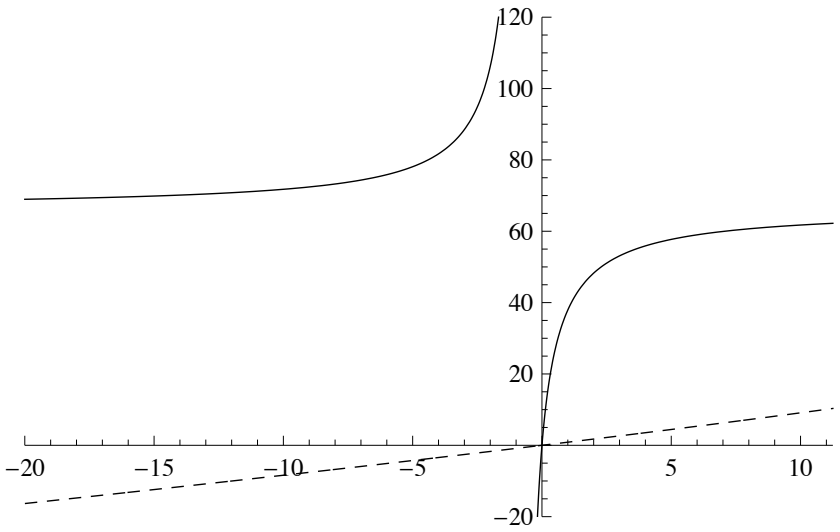

Figure 3.4: Relative contributions of $A_p(w)$ (solid line) and $A_\sigma(w)$ (dashed line) to the amplitude $A(w)$ at $w \leqslant 11.25$.

to label the points x of 1+1 Minkowski space-time. The relevant solution is Lorentz-invariant, i.e., the functions $\varphi(\mathrm{z}, \bar{\mathrm{z}})$ and $\chi(\mathrm{z}, \bar{\mathrm{z}})$ depend only on the Lorentz-invariant combination $\rho = \mathrm{z}\bar{\mathrm{z}} = \mathrm{x}^2 - \mathrm{t}^2$. In this case (3.42) reduces to the ordinary differential equation, the famous Penlevé III equation. The solution we are interested in is specified by the asymptotic form as $\rho \to 0$,

$$\varphi(\rho) = -\frac{1}{2}\log(\rho/4) - \log(-\Omega) + O(\rho^2\Omega^2), \tag{3.44a}$$

$$\chi(\rho) = \frac{1}{4}\log(16\rho) + \log(-\Omega) + O(\rho), \tag{3.44b}$$

where

$$\Omega = \frac{1}{2}\log(\kappa^2\rho). \tag{3.45}$$

Under the special choice of the constant $\kappa = e^{\gamma_E}/8$, which we use, the solution $\varphi(\rho)$ is regular at all real ρ and decays as

$$\varphi(\rho) = \frac{2}{\pi}K_0(\sqrt{\rho}) + O\left(e^{-3\sqrt{\rho}}\right) \tag{3.46}$$

as $\rho \to +\infty$ [38]. The solution $\varphi(\rho)$ can be regarded as a function of the complex ρ. Using, e.g., the representation in [38], it is possible to show that $\varphi(\rho)$ is analytic in the whole ρ-plane with the branch cut from $-\infty$ to 0, except for the point $\rho = 0$ where the

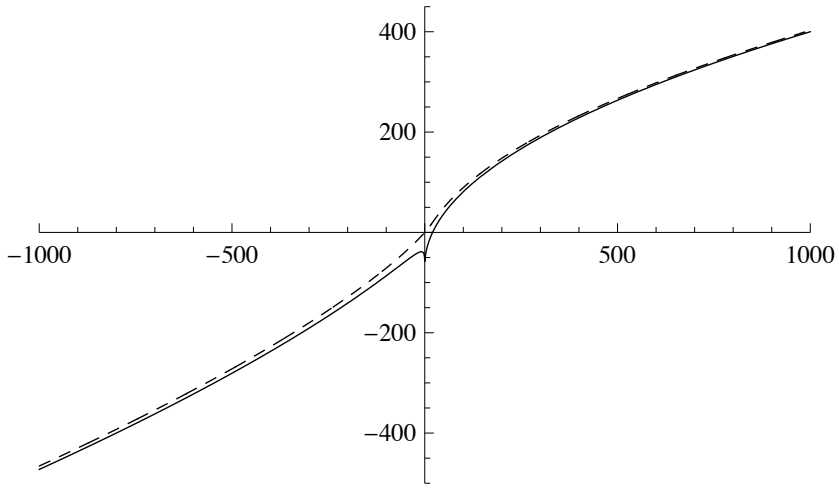

Figure 3.5: The real part of the amplitude at large w; the dashed line corresponds to $A_\sigma(w)$, the solid line shows its large-w asymptotic.

logarithmic singularity, explicit in (3.44), is located. Moreover, the asymptotic form (3.46) holds for $-\pi < \arg\rho < \pi$ as $|\rho| \to \infty$. The function $\chi(\rho)$ has similar analyticity, except that at large $|\rho|$ it tends to a constant

$$\chi(\rho) = 4\log\bar{s} + O\left(e^{-2\sqrt{\rho}}\right) \tag{3.47}$$

as $|\rho| \to \infty$, $-\pi < \arg\rho < \pi$, here $\bar{s}$ is a constant defined in (1.7). In the high-T regime, when $\langle\sigma\rangle = 0$ and $\langle\mu\rangle = \bar{\sigma}$, in the $h = 0$ IFT the correlation functions $G(\rho)$ and $\tilde{G}(\rho)$ are written in terms of $\varphi(\rho)$ and $\chi(\rho)$ as follows

$$G(\rho) = e^{\chi/2}\sinh(\varphi/2), \quad \tilde{G}(\rho) = e^{\chi/2}\cosh(\varphi/2). \tag{3.48}$$

Both correlation functions are real at space-like separations $\rho > 0$, while in the time-like domain the values at the upper edge of the branch cut, i.e., $G(\rho + i0)$ and $\tilde{G}(\rho + i0)$, have to be taken.

This relation can be extended to matrix elements of the products $T\sigma(x)\sigma(0)$ and $T\mu(x)\mu(0)$ inserted between any particle states. The main ingredient here is the special solution $\Psi_\pm(\mathrm{z}, \bar{\mathrm{z}}|\beta)$ of the linear system

$$\partial_{\mathrm{z}}\Psi_+ = -\frac{1}{2}\,\partial_{\mathrm{z}}\varphi\,\Psi_+ + \frac{e^\beta}{4}\,e^{\varphi}\,\Psi_-, \tag{3.49a}$$

$$\partial_{\mathrm{z}}\Psi_- = \frac{1}{2}\,\partial_{\mathrm{z}}\varphi\,\Psi_- - \frac{e^\beta}{4}\,e^{-\varphi}\,\Psi_+, \tag{3.49b}$$

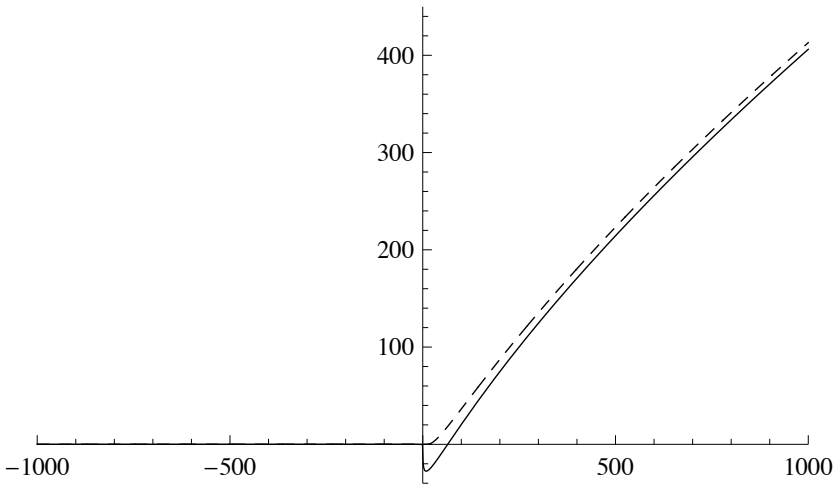

Figure 3.6: The imaginary part of the amplitude at large w; the dashed line corresponds to $A_\sigma(w)$, the solid line shows its large-w asymptotic.

and

$$\partial_{\bar{\mathrm{z}}}\Psi_+ = \frac{1}{2}\,\partial_{\bar{\mathrm{z}}}\varphi\,\Psi_+ - \frac{e^{-\beta}}{4}\,e^{-\varphi}\,\Psi_-, \tag{3.50a}$$

$$\partial_{\bar{\mathrm{z}}}\Psi_- = -\frac{1}{2}\,\partial_{\bar{\mathrm{z}}}\varphi\,\Psi_- + \frac{e^{-\beta}}{4}\,e^{\varphi}\,\Psi_+, \tag{3.50b}$$

which constitutes the Lax representation of the sinh-Gordon equation (the first of the equations (3.42) guarantees integrability of (3.49a) and (3.50a)) with e^β playing the role of the spectral parameter. The solution $\Psi_\pm(x|\beta)$, relevant to our problem, is described in some detail in [10][8]. The components $\Psi_\pm(x|\beta)$ are analytic functions on the double cover of the Minkowski space-time parametrized by the coordinates $x = (\mathrm{z}, \bar{\mathrm{z}})$, with the branching singularities at the right and left parts of the light cone, i.e., at $\mathrm{z} = 0$ and $\bar{\mathrm{z}} = 0$. The double cover is needed because $\Psi_\pm(x|\beta)$ change sign when the point x is brought around the origin $(\mathrm{z}, \bar{\mathrm{z}}) = (0, 0)$.

Due to the obvious symmetry of (3.49a) and (3.50a), the functions $\Psi_\pm(x|\beta)$ depend only on the combinations $Z = e^\beta\,\mathrm{z}$, $\bar{Z} = e^{-\beta}\,\bar{\mathrm{z}}$, and below we often use the notation $\Psi_\pm(Z, \bar{Z})$ for them. The solution under consideration can be characterized by its

[8]In [10] this solution is described in the Euclidean space, where $\mathrm{z} = \mathrm{x} + i\mathrm{y}$, $\bar{\mathrm{z}} = \mathrm{x} - i\mathrm{y}$. Here we discuss its continuation $\mathrm{y} \to i\mathrm{t}$. The continuation is straightforward for space-like separations $\rho > 0$. In the time-like domains $\rho < 0$, the standard $i0$ prescription $\mathrm{z} \to \mathrm{z} + i0\,\mathrm{sign}(\bar{\mathrm{z}})$, $\bar{\mathrm{z}} \to \bar{\mathrm{z}} + i0\,\mathrm{sign}(\mathrm{z})$ is implied.

behavior as $(Z, \bar{Z}) \to \infty$,

$$\Psi_+(Z,\bar{Z}) = \sqrt{\frac{\pi}{-\Omega}}\left(\frac{Z}{\bar{Z}}\right)^{1/4}\left[1+\frac{4\Omega-1}{64}\bar{Z}^2-\frac{1}{64}Z^2+O(\rho^4\Omega^2)\right], \tag{3.51a}$$

$$\Psi_-(Z,\bar{Z}) = \sqrt{\frac{\pi}{-\Omega}}\left(\frac{\bar{Z}}{Z}\right)^{1/4}\left[1+\frac{4\Omega-1}{64}Z^2-\frac{1}{64}\bar{Z}^2+O(\rho^4\Omega^2)\right], \tag{3.51b}$$

where Ω is defined in (3.45).

The matrix elements of the T-product of $\sigma(x)\sigma(0)$ between particle states are certain products of the functions $\Psi_\pm(x|\beta)$. The relation looks somewhat simpler for the "centered" product $T\sigma(x/2)\sigma(-x/2)$; the integral (3.26) is clearly insensitive to this shift. First, define the two-particle matrix elements

$$\mathcal{G}(\theta,\theta') = \langle 0|T\sigma(x/2)\sigma(-x/2)|\theta,\theta'\rangle, \tag{3.52a}$$

$$\mathcal{G}(\theta|\theta') = \langle \theta|T\sigma(x/2)\sigma(-x/2)|\theta'\rangle - 2\pi\delta(\theta-\theta')G, \tag{3.52b}$$

where $G = G(\rho)$ is one of the two-point functions in (3.48), and we omit the argument x in $\mathcal{G}(\theta,\theta')$ and $\mathcal{G}(\theta|\theta')$ to simplify notations. Then we have

$$\mathcal{G}(\theta_1,\theta_2) = -\frac{i}{2}\left[G\frac{e^{\theta_1}-e^{\theta_2}}{e^{\theta_1}+e^{\theta_2}}\Psi_s(\theta_1,\theta_2)-\tilde{G}\Psi_a(\theta_1,\theta_2)\right], \tag{3.53a}$$

$$\mathcal{G}(\theta_1|\theta_2) = -\frac{1}{2}\left[G\frac{e^{\theta_1}+e^{\theta_2}}{e^{\theta_1}-e^{\theta_2}}\Psi_a(\theta_1,\theta_2)-\tilde{G}\Psi_s(\theta_1,\theta_2)\right], \tag{3.53b}$$

where $\tilde{G}$ is the other two-point function in (3.48), and

$$\Psi_s(\theta_1,\theta_2) = \Psi_+(Z_1,\bar{Z}_1)\Psi_-(Z_2,\bar{Z}_2)+\Psi_-(Z_1,\bar{Z}_1)\Psi_+(Z_2,\bar{Z}_2), \tag{3.54a}$$

$$\Psi_a(\theta_1,\theta_2) = \Psi_+(Z_1,\bar{Z}_1)\Psi_-(Z_2,\bar{Z}_2)-\Psi_-(Z_1,\bar{Z}_1)\Psi_+(Z_2,\bar{Z}_2). \tag{3.54b}$$

Here

$$(Z_1,\bar{Z}_1) = (e^{\theta_1}\mathrm{z}, e^{-\theta_1}\bar{\mathrm{z}}), \quad (Z_2,\bar{Z}_2) = (e^{\theta_2}\mathrm{z}, e^{-\theta_2}\bar{\mathrm{z}}).$$

Finally, the four-particle matrix element in (3.26) is the fermionic Wick product of the two-particle matrix element (3.53),

$$\begin{aligned}\langle\theta_1,\theta_2|T\sigma(x/2)\sigma(-x/2)|\theta_1,\theta_2\rangle_{conn} = \\ = G^{-1}\left[\mathcal{G}(\theta_2|\theta_1)\mathcal{G}(\theta_1|\theta_2)-\mathcal{G}(\theta_1|\theta_1)\mathcal{G}(\theta_2|\theta_2)+\mathcal{G}(\theta_1,\theta_2)\mathcal{G}(\theta_1,\theta_2)\right].\end{aligned} \tag{3.55}$$

It will be convenient to write $\mathcal{G}(\theta|\theta)$, which is simply the limit of $\mathcal{G}(\theta|\theta')$ as $\theta' \to \theta$, as the sum of two terms

$$\mathcal{G}(\theta|\theta) = \tilde{G}\, K(Z,\bar{Z}) - G\, L(Z,\bar{Z}), \tag{3.56}$$

where

$$K(Z,\bar{Z}) = \Psi_+(Z,\bar{Z})\Psi_-(Z,\bar{Z}), \tag{3.57a}$$

$$L(Z,\bar{Z}) = \Psi_-(Z,\bar{Z})\partial_\theta\Psi_+(Z,\bar{Z}) - \Psi_+(Z,\bar{Z})\partial_\theta\Psi_-(Z,\bar{Z}), \tag{3.57b}$$

and again $Z = e^{\theta}\mathrm{z}$, $Z = e^{-\theta}\bar{\mathrm{z}}$.

3.3.2 High-energy limit of the integral (3.26)

The expression for the matrix element in (3.26) described above is still too complicated for the integral to be evaluated in closed form. However, it is possible to use this representation to derive its limiting behavior as $\theta_{12} \to \infty$.

To simplify arguments, we assume that $\theta_1 \to +\infty$ and $\theta_2 \to -\infty$. In this limit the factors involving the ratio $e^{\theta_1} - e^{\theta_2}$ and $e^{\theta_1} + e^{\theta_2}$ in (3.53) can be dropped, and the expression (3.55) simplifies as

$$\begin{aligned}\langle\theta_1,\theta_2|T\sigma(x/2)\sigma(-x/2)|\theta_1,\theta_2\rangle_{conn} \to G\left[K(Z_1,\bar{Z}_1)K(Z_2,\bar{Z}_2)+\right.\\ \left.+L(Z_1,\bar{Z}_2)L(Z_2,\bar{Z}_2)\right] - \tilde{G}\left[K(Z_1,\bar{Z}_1)L(Z_2,\bar{Z}_2) + L(Z_1,\bar{Z}_2)K(Z_2,\bar{Z}_2)\right],\end{aligned} \tag{3.58}$$

where K and L are the functions (3.57). Furthermore, it is possible to show that at $|Z+\bar{Z}| \gg 1$ the functions $\Psi_\pm(Z,\bar{Z})$ approach plane waves. The exact form of the plane waves is different for different regions in the $(Z,\bar{Z})$-plane. Thus, as $Z \to +\infty$, $Z \gg \bar{Z}$, we have

$$\Psi_+(Z,\bar{Z}) \to 2\, e^{\varphi/2}\cos\left(\frac{Z-\bar{Z}}{4} - \frac{\pi}{4}\right), \tag{3.59a}$$

$$\Psi_-(Z,\bar{Z}) \to 2\, e^{-\varphi/2}\cos\left(\frac{Z-\bar{Z}}{4} + \frac{\pi}{4}\right), \tag{3.59b}$$

while as $\bar{Z} \to +\infty$, $\bar{Z} \gg Z$,

$$\Psi_+(Z,\bar{Z}) \to 2\, e^{-\varphi/2}\cos\left(\frac{Z-\bar{Z}}{4} - \frac{\pi}{4}\right), \tag{3.60a}$$

$$\Psi_-(Z,\bar{Z}) \to 2\, e^{\varphi/2}\cos\left(\frac{Z-\bar{Z}}{4} + \frac{\pi}{4}\right). \tag{3.60b}$$

When $Z \sim \bar{Z} \to +\infty$ the difference between (3.59) and (3.60) is irrelevant since in this domain $\varphi \to 0$. Likewise, as $Z \to -\infty$, $-Z \gg \bar{Z}$,

$$\Psi_+(Z,\bar{Z}) \to 2i\, e^{\varphi/2} \cos\left(\frac{Z-\bar{Z}}{4} + \frac{\pi}{4}\right), \tag{3.61a}$$

$$\Psi_-(Z,\bar{Z}) \to -2i\, e^{-\varphi/2} \cos\left(\frac{Z-\bar{Z}}{4} - \frac{\pi}{4}\right), \tag{3.61b}$$

while as $\bar{Z} \to -\infty$, $-\bar{Z} \gg Z$,

$$\Psi_+(Z,\bar{Z}) \to 2i\, e^{-\varphi/2} \cos\left(\frac{Z-\bar{Z}}{4} + \frac{\pi}{4}\right), \tag{3.62a}$$

$$\Psi_-(Z,\bar{Z}) \to -2i\, e^{\varphi/2} \cos\left(\frac{Z-\bar{Z}}{4} - \frac{\pi}{4}\right). \tag{3.62b}$$

In writing these equations we have ignored the overall sign ambiguity of $\Psi_\pm$ (if the sign is fixed as in (3.59) and (3.60), the overall signs in (3.61) and (3.62) still depend on the way of continuation around the point $(Z,\bar{Z}) = (0,0)$), because this ambiguity does not affect the functions (3.57). From these equations one finds the corresponding asymptotics for the functions (3.57),

$$K(Z,\bar{Z}) \to 2\cos\left(\frac{Z-\bar{Z}}{2}\right), \quad L(Z,\bar{Z}) \to |Z+\bar{Z}| \tag{3.63}$$

as $|Z+\bar{Z}| \to \infty$.

The leading $\theta_{12} \to \infty$ asymptotic of the integral (3.26) clearly comes from the term with $G\,L(Z_1,\bar{Z}_1)L(Z_2,\bar{Z}_2)$ in (3.58). The remaining terms involve the fast oscillating function K, and integration over $(\mathrm{z},\bar{\mathrm{z}})$ leads to their suppression by at least one power of $e^{-\theta_{12}}$, as compared to the leading term. The leading high-energy asymptotic $\theta_{12} \to \infty$ of the amplitude (3.26) is thus given by

$$iA(\theta_{12}) \to -\frac{1}{2}\int d^2x\, |UV|\, G(\rho + i0), \quad \theta_{12} \to +\infty, \tag{3.64}$$

where $d^2x = d\mathrm{x}d\mathrm{t} = \frac{1}{2}dzd\bar{\mathrm{z}}$, and

$$U = Z_1 + \bar{Z}_1 = e^{\theta_1}\mathrm{z} + e^{-\theta_1}\bar{\mathrm{z}}, \quad V = Z_2 + \bar{Z}_2 = e^{\theta_2}\mathrm{z} + e^{-\theta_2}\bar{\mathrm{z}}. \tag{3.65}$$

The integral here can be handled as follows. Write

$$|UV| = UV - 2UV\,\Theta(-UV), \tag{3.66}$$

where $\Theta(x)$ is the usual step function. The first term in the integral is analytic in the coordinates $(\mathrm{z}, \bar{\mathrm{z}})$, and its contribution can be evaluated using the Wick rotation, $\mathrm{t} \to -i\mathrm{y}$, yielding

$$-\frac{1}{2}\int d^2x\, UV G(\mathrm{z}\bar{\mathrm{z}}) \to \pi\, i\, G^{(3)} \exp(\theta_{12}), \tag{3.67}$$

where

$$G^{(3)} = \frac{1}{2}\int_0^\infty \rho\, G(\rho) d\rho \tag{3.68}$$

is the third moment of the Euclidean spin-spin correlation function. The second term in (3.66) involves the step function which limits the integration domain to $UV > 0$. In the domain $U < 0$, $V > 0$, which lies entirely within the future light-cone $\rho = \mathrm{z}\bar{\mathrm{z}} < 0$, $\mathrm{z} < 0$, one can parametrize $\mathrm{z} = -\sqrt{-\rho}\, e^{-\phi}$, $\bar{\mathrm{z}} = \sqrt{-\rho}\, e^{\phi}$, with the integration domain corresponding to the range $\theta_2 < \phi < \theta_1$ of the Lorentz parameter ϕ. Therefore, at $\theta_{12} \gg 1$ the contribution from this domain to the integral in (3.64) is

$$\int_{U<0<V} UV\, G(\rho + i0) d^2x \approx -\theta_{12} \exp(\theta_{12}) \int_{-\infty}^0 \rho\, G(\rho + i0) d\rho = \\ = \theta_{12} \exp(\theta_{12}) \int_0^\infty \rho\, G(\rho) d\rho, \tag{3.69}$$

where the last form is obtained by rotating the integration contour $\rho \to e^{-i\pi}\rho$, which is possible since $G(\rho)$ decays exponentially into the upper half-plane of complex ρ. The "past" part of the light-cone $\mathrm{z} > 0 > \bar{\mathrm{z}}$ brings in an identical contribution. Collecting all these pieces together, we have

$$\frac{iA(\theta_{12})}{\sinh\theta_{12}} \to -4\, G^{(3)} \left[\theta_{12} - i\pi/2 + \theta_0\right], \tag{3.70}$$

where θ_0 is a real constant whose value cannot be determined by the simple analysis above, its calculation would require much better understanding of the behavior $L(Z, \bar{Z})$ in the domain $Z + \bar{Z} \sim 1$.

The asymptotic (3.70) can be written in terms of the variable (3.17) as

$$iA(w + i0) \to -2G^{(3)}\sqrt{w}\left[\log(w/w_0) - i\pi\right], \quad w \to +\infty, \tag{3.71}$$

with w_0 being a real positive constant related to θ_0. This equation can be extended to the whole complex w-plane with the branch cut along the positive part of the real axis,

$$A(w) \to -2G^{(3)}\sqrt{-w}\log(-w/w_0), \quad |w| \to \infty, \quad -\pi < \arg(-w) < \pi, \tag{3.72}$$

where the branch of the multi-valued function is chosen in such a way that $\sqrt{-w}$ is positive and $\log(-w)$ is real at real negative w. From (3.23) one finds the high-energy behavior of the h^2-term in the inelastic cross-section,

$$\sigma_{tot}^{(2)}(w) \to 4\,G^{(3)}\log(w/w_0) \approx 8G^{(3)}\log(E^2), \tag{3.73}$$

which is of the same logarithmic form as the high-energy behavior of $\sigma_{2\to 3}^{(2)}$, determined in Section 3.2, the equation (3.40). Note that the coefficient in (3.40) corresponds to the one-particle contribution $G_{1P}(\rho) = (1/\pi)K_0(\sqrt{\rho})$ in the intermediate-state decomposition of the spin-spin correlation function $G(\rho)$,

$$\frac{1}{2}\int_0^\infty \rho\, G_{1P}(\rho)\, d\rho = \frac{4\bar{\sigma}^2}{\pi} = 2.3475035314\ldots \tag{3.74}$$

Comparing the exact value of $G^{(3)}$,

$$G^{(3)} = \int_0^\infty r^3\langle\sigma(r)\sigma(0)\rangle\, dr = 2.34752921866\ldots, \tag{3.75}$$

and the one-particle contribution (3.74) reaffirms the statement that $\sigma_{tot}^{(2)}$ is dominated by its three-particle component $\sigma_{2\to 3}^{(2)}$.

3.4 Remarks about higher orders in h^2

The logarithmic growth with the energy in (3.73) of the h^2-term in the inelastic cross-section,

$$\sigma_{tot} \to 8G^{(3)}h^2\log(E^2) + O(h^4), \tag{3.76}$$

suggests that the higher-order terms of the h^2-expansion become significant at high energies, since unitarity requires $\sigma_{tot} \leqslant 1$ at all energies. One can expect that the terms of the higher order h^{2n} in the expansion (3.24) are $\sim h^{2n}\log^n E^2$ at large E. Here we argue that it is indeed so, and, moreover, that summing up these leading logarithms results in a power-like behavior[9]

$$\sigma_{tot} \to 1 - (E/E_0)^{-\alpha} \quad \text{as } E \to \infty, \tag{3.77}$$

[9]This behavior, with $\alpha \approx 64(\bar{\sigma}h)^2/\pi$, was earlier proposed, on the basis of a different argument, by S. Rutkevich [40]. He also suggested the high-energy form of the partial cross-sections $\sigma_{2\to 2+n} \approx (1/n!)(\alpha\log(E/E_0))^n(E/E_0)^{-\alpha}$.

where $\alpha \approx 16G^{(3)}(\bar{\sigma}h)^2$ at small h^2, and $E_0 = C\,m$, with the yet unknown constant C.

First, let us note that the expression (3.64) admits a simple, essentially classical interpretation as follows. Let us introduce coordinates

$$(u, v) = (e^{\theta_1}\,\mathrm{z} + e^{-\theta_1}\,\bar{\mathrm{z}}, e^{\theta_2}\,\mathrm{z} + e^{-\theta_2}\,\bar{\mathrm{z}}) \tag{3.78}$$

on the $(\mathrm{z}, \bar{\mathrm{z}})$-plane, and assume that at $\theta_{12} \to \infty$ the particles with the rapidities θ_1 and θ_2 can be represented by their classical trajectories $u = 0$ and $v = 0$, respectively. Also assume that unless the points x_1, x_2 are too close to the trajectories, the matrix element $\langle\theta_1, \theta_2|T\sigma(x_1)\sigma(x_2)|\theta_1, \theta_2\rangle$ is approximated by the correlation function $\langle 0|T\sigma(x_1)\sigma(x_2)|0\rangle$, multiplied by the sign factor which depends on whether the insertion points x_1 and x_2 are located on the same side or on different sides of each of the trajectories. More specifically, we assume[10]

$$\begin{aligned}\langle\theta_1, \theta_2|T\sigma(x_1)\sigma(x_2)|\theta_1, \theta_2\rangle \approx \\ \approx \mathrm{sign}(u_1)\,\mathrm{sign}(u_2)\,\mathrm{sign}(v_1)\,\mathrm{sign}(v_2)\langle 0|T\sigma(x_1)\sigma(x_2)|0\rangle,\end{aligned} \tag{3.79}$$

where (u_1, v_1) and (u_2, v_2) are the coordinates (3.78) of the points x_1 and x_2, respectively[11]. This expression still involves the "disconnected" parts,

$$[1 + (\mathrm{sign}(u_1)\,\mathrm{sign}(v_1) - 1) + (\mathrm{sign}(u_2)\,\mathrm{sign}(v_2) - 1)]\langle 0|T\sigma(x_1)\sigma(x_2)|0\rangle.$$

Subtracting these, one obtains

$$\langle\theta_1, \theta_2|T\sigma(x_1)\sigma(x_2)|\theta_1, \theta_2\rangle_{conn} \approx 4\Theta(-u_1v_1)\Theta(-u_2v_2)\langle 0|T\sigma(x_1)\sigma(x_2)|0\rangle, \tag{3.80}$$

where $\Theta(u)$ is again the usual step function. Since the two-point correlation function $\langle 0|T\sigma(x_1)\sigma(x_2)|0\rangle$ depends only on the separation $x_1 - x_2$, one can explicitly integrate

[10] To simplify notations, here and below we ignore the delta-functions associated with the plane-wave normalization (3.2) of the particle states. Instead, one can think of normalized wave packets centered at the rapidities θ_1 and θ_2.

[11] Similar approximation was put forward in a different context in [39]. In our case it can be justified as follows. The correlation between the spin operators located at the points x_1 and x_2 is due to exchanges of an odd number of particles. An external particle trajectory which passes between these two points intersects an odd number of the trajectories of these exchange particles, thus producing the minus sign.

out one of the coordinates in

$$\frac{1}{2}\int d^2x_1 d^2x_2\, \langle\theta_1,\theta_2|T\sigma(x_1)\sigma(x_2)|\theta_1,\theta_2\rangle_{conn} = \\ = -\frac{1}{2\sinh\theta_{12}}\int d^2x\, |UV|\langle 0|T\sigma(x/2)\sigma(-x/2)|0\rangle, \quad (3.81)$$

where $U = u_1 - u_2$, $V = v_1 - v_2$ are the coordinates (3.78) associated with the separation $x = x_1 - x_2$. The last expression is equivalent to (3.67), which leads to the logarithmic behavior (3.71). The origin of the logarithm is clear. Apart from the step function, the integrand in (3.81) is Lorentz-invariant. The step function provides the cutoff for the integration over the Lorentz boost parameter ϕ in the integral over $d^2x = d\rho\, d\phi$. Thus, the term $\theta_{12} \approx \frac{1}{2}\log w$ in (3.70) is just the size of the Lorentz boost which brings the rest frame of the particle 2 to the rest frame of the particle 1.

The same approximation can be applied to the higher-order terms in the perturbative expansion of

$$S(\theta_{12}) = -\langle\theta_1,\theta_2|\, T\exp\left(-ih\int\sigma(x)d^2x\right)|\theta_1,\theta_2\rangle_{conn} \quad (3.82)$$

by assuming that at $\theta_{12}\to\infty$ one can write

$$\langle\theta_1,\theta_2|\, T\sigma(x)\sigma(x_2)\ldots\sigma(x_{2n})|\theta_1,\theta_2\rangle \to \\ \to \left[\prod_{i=1}^{2n}\mathrm{sign}(u_i)\,\mathrm{sign}(v_i)\right]\langle 0|\, T\sigma(x)\sigma(x_2)\ldots\sigma(x_{2n})|0\rangle, \quad (3.83)$$

where (u_i, v_i) are the coordinates (3.78) of the points x_i. Again, apart from the sign factors $\mathrm{sign}(u_i)\,\mathrm{sign}(v_i)$, the right-hand side of (3.83) is invariant with respect to simultaneous Lorentz transformations of the coordinates x_i. Therefore, integration over $\prod_{i=1}^{2n} d^2x_i$ generates at least one factor θ_{12}. But in fact this integration produces much larger contribution $\sim\theta_{12}^n$. Indeed, the $2n$-point correlation function contains $(2n)!/(2^n n!)$ fully disconnected terms

$$\langle 0|T\sigma(x_1)\sigma(x_2)|0\rangle\langle 0|T\sigma(x_3)\sigma(x_4)|0\rangle\ldots\langle 0|T\sigma(x_{2n-1})\sigma(x_{2n})|0\rangle + \text{permutations}. \quad (3.84)$$

These terms are invariant with respect to n copies of the Lorentz group, each acting on a respective pair of the points. Because of the factorization, these terms can be handled

exactly as it was done before with the h^2-contribution, and it leads to the contribution $\sim (h^2\theta_{12})^n$ to (3.82). It is not difficult to see that the contributions from the fully disconnected terms above form an exponential series in $h^2\,\theta_{12} \sim h^2 \log w$. Assuming that there are no other sources of such "leading logarithms", which clearly needs to be proven by a more detailed analysis, this suggests the power-like decay of the $2 \to 2$ S-matrix element in terms of the variable (3.17)

$$S(w) \sim (-w/w_0)^{-2G^{(3)}h^2} \tag{3.85}$$

as $|w| \to \infty$, $-\pi < \arg w < \pi$. Here again we choose the branch of the function in such a way that $S(w)$ is real at negative w. This corresponds to the behavior (3.77) of the inelastic cross-section.

Finally, we note that the asymptotic behavior (3.85) agrees with naive "two-particle" unitarization of (3.20),

$$S(\theta) = -\frac{\sinh\theta + i\sin(2\pi/3)}{\sinh\theta - i\sin(2\pi/3)}\frac{\sinh\theta - i\sin(2\pi/3 + rh^2)}{\sinh\theta + i\sin(2\pi/3 + rh^2)}\exp\left(\frac{ih^2 A_\sigma(\theta)}{\sinh\theta}\right), \tag{3.86}$$

where $r = 36\bar{\sigma}^2$, and $A_\sigma(\theta)$ is the second term in (3.25). Although (3.86) involves all powers of h^2, it is, of course, not the exact expression for the $2 \to 2$ S-matrix element, since it ignores the higher-order corrections to the residue (3.33), as well as the higher-order terms in σ_{tot}.

3.5 Discussion

In this chapter we use two different methods to compute high-energy asymptotic for the scattering amplitude. What we observe is that to the first order in h^2 the amplitude is dominated by the logarithmic term

$$S \to -1 + 8h^2 G^{(3)}\left[\log(E/E_0) - i\pi/4\right] + O(h^4) \tag{3.87}$$

as E, the center-of-mass energy, goes to infinity. Here $G^{(3)}$ is the third moment of the spin-spin correlation function[12]

$$G^{(3)} = \int_0^\infty r^3 \langle\sigma(r)\sigma(0)\rangle dr = (2.34752921866\ldots)\, m^{-15/4}. \tag{3.88}$$

[12]Here we restore the mass to give an idea of the dimensionality of the expression.

The asymptotic behavior (3.87) indicates the logarithmic growth of the leading term in the h^2-expansion of the total inelastic cross-section. The unitarity bound $\sigma_{tot} \leqslant 1$ suggests that (3.87) represents but the first terms of a series in the "leading logarithms" $(h^2 \log E)^n$. We presented an argument in support of this statement which also shows that the leading logarithms form an exponential series that gives a power-like decay $|S_{2\to 2}| \sim E^{-8G^{(3)}h^2}$ at large E. This behavior suggests that while at low energies the two-particle scattering is dominated by the elastic $2 \to 2$-channel, at large E the scattering goes almost entirely through inelastic channels, even at small h^2.

These results are somewhat disappointing from the following point of view. We know that as η grows from $-\infty$, the particle spectrum of the IFT changes qualitatively: at $\eta \approx -2.09$ the second stable particle with the mass M_2 appears in the spectrum in addition to the first particle, the third particle becomes stable at $\eta \approx -0.14$, and this process of particle multiplication continues further with growing η (Fig. 1.3). Therefore, at sufficiently large negative η, when we have a single stable particle in the theory, we would expect other particles, or at least the lighter ones, to exist in form of resonances that should be observable in the amplitude at sufficiently high energies, and this does not seem to be the case, at least at the current level of understanding. There are two possible scenarios that could resolve this puzzle. The first one is that at $h^2 \to 0$ the resonance masses when taken in units of m, the lightest stable particle, depart to infinity in a non-analytic manner, e.g., as $M_{res}^2 \sim e^{C/h^2}$, where C is a certain constant. This would indicate that the point $h = 0$, while being just a regular point for the vacuum energy, becomes an essential singularity when the particle masses are considered. Another possibility is that the resonances disappear at infinity at certain positive values of E^{-h^2}. In any case, the work presented here has to be considered as just the beginning of the systematic analysis of scattering in the high-temperature IFT.

References

[1] A. A. Belavin, A. M. Polyakov and A. B. Zamolodchikov, "Infinite conformal symmetry in two-dimensional quantum field theory," Nucl. Phys. B **241**, 333 (1984).

[2] C. Itzykson, J.-M. Drouffe, "Statistical field theory," Cambridge University Press, 1989.

[3] T. T. Wu, B. M. McCoy, "The two-dimensional Ising model," Harvard University Press, 1973.

[4] B. M. McCoy and T. T. Wu, "Two-dimensional Ising field theory in a magnetic field: breakup of the cut in the two-point function," Phys. Rev. D **18**, 1259 (1978).

[5] A. B. Zamolodchikov, "Integrals of motion and S-matrix of the (scaled) $T = T_c$ Ising model with magnetic field," Int. J. Mod. Phys. A **4**, 4235 (1989).

A. B. Zamolodchikov, "Integrable field theory from conformal field theory," Adv. Stud. Pure Math. **19**, 641 (1989).

[6] A. B. Zamolodchikov and A. B. Zamolodchikov, "Factorized S-matrices in two dimensions as the exact solutions of certain relativistic quantum field models," Annals Phys. **120**, 253 (1979).

[7] G. Mussardo, "Off-critical statistical models: factorized scattering theories and bootstrap program," Phys. Rept. **218**, 215 (1992).

[8] G. Delfino, G. Mussardo and P. Simonetti, "Non-integrable quantum field theories as perturbations of certain integrable models," Nucl. Phys. B **473**, 469 (1996); arXiv:hep-th/9603011.

[9] P. Fonseca and A. Zamolodchikov, "Ising field theory in a magnetic field: Analytic properties of the free energy," J. Stat. Phys. 110, 527 (2003); arXiv:hep-th/0112167.

[10] P. Fonseca and A. Zamolodchikov, "Ward identities and integrable differential equations in the Ising field theory," arXiv:hep-th/0309228.

[11] S. B. Rutkevich, "Large-n excitations in the ferromagnetic Ising field theory in a small magnetic field: mass spectrum and decay widths," Phys. Rev. Lett. **95**, 250601 (2005); arXiv:hep-th/0509149.

[12] G. Delfino, P. Grinza and G. Mussardo, "Decay of particles above threshold in the Ising field theory with magnetic field," Nucl. Phys. B **737**, 291 (2006); arXiv:hep-th/0507133.

[13] P. Fonseca and A. Zamolodchikov, "Ising spectroscopy I: mesons at $T < T_c$," arXiv:hep-th/0612304.

[14] S. B. Rutkevich, "Form-factor perturbation expansions and confinement in the Ising field theory," J. Phys. A **42**, 304025 (2009); arXiv:0901.157 [cond-mat.stat-mech].

[15] R. Peierls, "On Ising's model of ferromagnetism," Proc. Camb. Philos. Soc. **32**, 477 (1936).

[16] L. Onsager, "Crystal statistics. 1. A two-dimensional model with an order disorder transition," Phys. Rev. **65**, 117 (1944).

[17] L. P. Kadanoff and H. Ceva, "Determination of an operator algebra for the two-dimensional Ising model," Phys. Rev. B **3**, 3918 (1971).

[18] C. N. Yang and T. D. Lee, "Statistical theory of equations of state and phase transitions. I: Theory of condensation," Phys. Rev. **87**, 404 (1952).

T. D. Lee and C. N. Yang, "Statistical theory of equations of state and phase transitions. II: Lattice gas and Ising model," Phys. Rev. **87**, 410 (1952).

[19] M. E. Fisher, "Yang-Lee edge singularity and φ^3-field theory," Phys. Rev. Lett. **40**, 1610 (1978).

[20] J. L. Cardy, "Conformal invariance and the Yang-Lee edge singularity in two dimensions," Phys. Rev. Lett. **54**, 1354 (1985).

[21] V. P. Yurov and A. B. Zamolodchikov, "Truncated conformal space approach to scaling Lee-Yang model," Int. J. Mod. Phys. A **5**, 3221 (1990).

[22] P. Grinza and A. Rago, "Study of the 2d Ising model with mixed perturbation," Nucl. Phys. B **651**, 387 (2003); arXiv:hep-th/0208016.

[23] M. Caselle, P. Grinza and A. Rago, "Amplitude ratios for the mass spectrum of the 2d Ising model in the high-T, $H \neq 0$ phase," J. Stat. Mech. **0410**, P009 (2004); arXiv:hep-lat/0408044.

[24] V. P. Yurov and A. B. Zamolodchikov, "Truncated fermionic space approach to the critical 2d Ising model with magnetic field," Int. J. Mod. Phys. A **6**, 4557 (1991).

[25] P. D. Fonseca, "Non-existence of local integrals of motion in the multi-deformed Ising model," Mod. Phys. Lett. A **13**, 1931 (1998); arXiv:hep-th/9804144.

[26] G. 't Hooft, "A two-dimensional model for mesons," Nucl. Phys. B **75**, 461 (1974).

[27] B. Berg, M. Karowski and P. Weisz, "Construction of Green functions from an exact S-matrix," Phys. Rev. D **19**, 2477 (1979).

[28] A. J. Hanson, R. D. Peccei and M. K. Prasad, "Two-dimensional $SU(N)$ gauge theory, strings and wings: comparative analysis of meson spectra and covariance," Nucl. Phys. B **121**, 477 (1977).

[29] S. Huang, J. W. Negele and J. Polonyi, "Meson structure in QCD in two dimensions," Nucl. Phys. B **307**, 669 (1988).

[30] R. L. Jaffe and P. F. Mende, "When is field theory effective?," Nucl. Phys. B **369**, 189 (1992).

[31] W. Krauth and M. Staudacher, "Non-integrability of two-dimensional QCD," Phys. Lett. B **388**, 808 (1996); arXiv:hep-th/9608122.

[32] I. Bars and M. B. Green, "Poincare and gauge invariant two-dimensional QCD," Phys. Rev. D **17**, 537 (1978).

[33] S. Coleman, "Aspects of symmetry," Cambridge University Press, 1985.

[34] R. Narayanan and H. Neuberger, "The quark mass dependence of the pion mass at infinite N," Phys. Lett. B **616**, 76 (2005); arXiv:hep-lat/0503033.

[35] V. A. Fateev, S. L. Lukyanov and A. B. Zamolodchikov, "On mass spectrum in 't Hooft's 2d model of mesons," J. Phys. A **42**, 304012 (2009); arXiv:0905.2280 [hep-th].

[36] I. Ziyatdinov, "Asymptotic properties of mass spectrum in 't Hooft's model of mesons," Int. J. Mod. Phys. A **25**, 3899 (2010); arXiv:1003.4304 [hep-th].

[37] R. J. Eden, P. V. Landshoff, D. I. Olive, J. C. Polkinghorne, "The analytic S-matrix," Cambridge University Press, 1966.

[38] T. T. Wu, B. M. McCoy, C. A. Tracy and E. Barouch, "Spin-spin correlation functions for the two-dimensional Ising model: exact theory in the scaling region," Phys. Rev. B **13**, 316 (1976).

[39] S. Sachdev, A. P. Young, "Low-temperature relaxation dynamics of the Ising chain in a transverse field," Phys. Rev. Lett. **78**, 2220 (1997); arXiv:cond-mat/9609185.

[40] S. Rutkevich, private communication.

[41] A. Zamolodchikov and I. Ziyatdinov, "Inelastic scattering and elastic amplitude in Ising field theory in a weak magnetic field at $T > T_c$. Perturbative analysis," arXiv:1102.0767 [hep-th].

[42] C. Itzykson and J. B. Zuber, "The planar approximation. 2," J. Math. Phys. **21**, 411 (1980).

M. L. Mehta, "A method of integration over matrix variables," Commun. Math. Phys. **79**, 327 (1981).

Appendix A

Computation of $\Delta_{odd/even}(\theta)$

In this appendix we sketch the computation of $\Delta_{odd}(\theta)$ and $\Delta_{even}(\theta)$, (2.35) and (2.36), respectively. For this first it is convenient to rewrite the wavefunctions (2.30) and (2.31) through more elementary functions

$$\varphi_+(\theta) = \frac{1}{2}\int_{-\infty}^{\infty} \frac{e^{iS(\beta)/\lambda}\, d\beta}{\sinh(\theta+\beta-i0)}, \quad \varphi_-(\theta) = \frac{1}{2}\int_{-\infty}^{\infty} \frac{e^{iS(\beta)/\lambda}\, d\beta}{\sinh(\theta-\beta+i0)}. \tag{A.1}$$

Then using $\varphi_+(-\theta) = -\varphi_-(\theta)$, we have

$$\varphi^{(0)}_{odd}(\theta) = \varphi_+(\theta) - \varphi_+(-\theta), \quad \varphi^{(0)}_{even}(\theta) = \varphi_+(\theta) + \varphi_+(-\theta). \tag{A.2}$$

Hence one has to evaluate $(\hat{H}-\alpha)\varphi_+(\theta)$ only, then separating the terms antisymmetric and symmetric with respect to the reflection $\theta \to -\theta$ gives the sought expressions.

It is useful to rewrite the operator $(\hat{H}-\alpha)$ as

$$(\hat{H}-\alpha)\varphi(\theta) = \cosh^2\theta\,(\hat{\Omega}+\hat{G})\varphi(\theta) \tag{A.3}$$

with

$$\hat{\Omega}\varphi(\theta) = \Omega(\theta)\varphi(\theta), \qquad \Omega(\theta) = -\frac{\partial S(\theta)}{\partial\theta} = 1 - \frac{\alpha}{\cosh^2\theta}, \tag{A.4}$$

and

$$\hat{G}\varphi(\theta) = -2\lambda \fint_{-\infty}^{\infty} \frac{d\theta'}{2\pi} \frac{\varphi(\theta')}{\sinh^2(\theta-\theta')}. \tag{A.5}$$

First, look at the integral

$$\hat{G}\varphi_+(\theta) = -\lambda \fint_{-\infty}^{\infty} \frac{d\theta'}{2\pi} \frac{1}{\sinh^2(\theta-\theta')} \int_{-\infty}^{\infty} \frac{e^{iS(\beta)/\lambda}\, d\beta}{\sinh(\theta'+\beta-i0)} =$$
$$= \lambda \frac{d}{d\theta} \fint_{-\infty}^{\infty} \frac{d\theta'}{2\pi} \coth(\theta-\theta') \int_{-\infty}^{\infty} \frac{e^{iS(\beta)/\lambda}\, d\beta}{\sinh(\theta'+\beta-i0)} =$$

One changes the order of integration. For fixed real β, shifting downward the contour of integration over θ', $\theta' = \alpha - i\pi/2$, produces an additional term coming from the pole of $\coth(\theta - \theta')$ at $\theta' = \theta$,

$$= i\lambda \frac{d}{d\theta} \int_{-\infty}^{\infty} \frac{d\beta}{2\pi}\, e^{iS(\beta)/\lambda} \int_{-\infty}^{\infty} d\alpha\, \frac{\tanh(\theta-\alpha)}{\cosh(\alpha+\beta)} + \frac{i\lambda}{2} \frac{d}{d\theta} \int_{-\infty}^{\infty} \frac{e^{iS(\beta)/\lambda}\, d\beta}{\sinh(\theta+\beta-i0)} =$$

The integral over α is evaluated in closed form

$$\int_{-\infty}^{\infty} d\alpha\, \frac{\tanh(\theta-\alpha)}{\cosh(\alpha+\beta)} = \pi \tanh \frac{\theta+\beta}{2}. \tag{A.6}$$

In the second integral, we change $d/d\theta$ to $d/d\beta$ and integrate by parts, thus getting the following

$$= \frac{i\lambda}{4} \int_{-\infty}^{\infty} d\beta\, \frac{e^{iS(\beta)/\lambda}}{\cosh^2 \frac{\theta+\beta}{2}} - \frac{1}{2} \int_{-\infty}^{\infty} \frac{\Omega(\beta)\, e^{iS(\beta)/\lambda}\, d\beta}{\sinh(\theta+\beta-i0)}. \tag{A.7}$$

One can notice that when plugged into (A.3) the term with $\Omega(\beta)$ combines with the term $\Omega(\theta)\varphi_+(\theta)$ giving

$$\frac{1}{2} \int_{-\infty}^{\infty} \frac{(\Omega(\theta) - \Omega(\beta))\, e^{iS(\beta)/\lambda}\, d\beta}{\sinh(\theta+\beta-i0)} = \frac{1}{2} \int_{-\infty}^{\infty} d\beta\, e^{iS(\beta)/\lambda}\, \frac{\alpha \sinh(\theta-\beta)}{\cosh^2\theta \cosh^2\beta}. \tag{A.8}$$

Hence, we get for (A.3)

$$(\hat{\Omega} + \hat{G})\varphi_+(\theta) = \frac{1}{2} \int_{-\infty}^{\infty} d\beta\, e^{iS(\beta)/\lambda} \left(\frac{\alpha \sinh(\theta-\beta)}{\cosh^2\theta \cosh^2\beta} + \frac{i\lambda}{2} \frac{1}{\cosh^2 \frac{\theta+\beta}{2}} \right). \tag{A.9}$$

Now this expression, appropriately anti-symmetrized and symmetrized, gives the formulae for $\Delta_{odd}(\theta)$ and $\Delta_{even}(\theta)$, (2.35) and (2.36), respectively.

Appendix B

Coordinate-space representation

Dependence of the terms in the low-energy expansion on roots of $\mathrm{Ai}'(-z)$ in (2.43) looks drastically different from the behavior in the odd sector. Therefore, it is worthwhile to provide another way to reproduce it.

In [9] a coordinate-space formulation for the bound-state equation was used to obtain the low-energy series for the spectrum of the IFT. Similarly we map 't Hooft's equation into the coordinate space. For simplicity we choose (2.25) as a starting point for our analysis. In $u = 2x - 1$, this equation becomes

$$\alpha\varphi(u) = \frac{\varphi(u)}{1-u^2} - 2\lambda \fint_{-1}^{1} \frac{\varphi(v)}{(u-v)^2}\frac{dv}{2\pi}. \tag{B.1}$$

Rescaling $u = tk$, $v = tp$, setting $\lambda = t^3$, expanding everything in t, and rearranging the terms, one gets

$$(1 - \alpha + t^2k^2 + t^4k^4 + \dots)\varphi(tk) = 2t^2 \fint_{-\infty}^{\infty} \frac{\varphi(tp)}{(p-k)^2}\frac{dp}{2\pi}. \tag{B.2}$$

Here we changed the limits of integration from $(-1/t, 1/t)$ to $(-\infty, \infty)$, an operation legitimate at $O(t^4)$.

Now this equation in the configuration space becomes

$$\left(-\varepsilon + |x| - \frac{d^2}{dx^2} + t^2\frac{d^4}{dx^4} - t^4\frac{d^6}{dx^6} + \dots\right)\psi(x) = 0. \tag{B.3}$$

Here the Fourier transform conventions in terms of the rescaled distance between quarks $x = t\,x_{real}$ are

$$\psi(x) = \int_{-\infty}^{\infty} \frac{dk}{2\pi}\, e^{ikx}\varphi(tk),$$

and we let $1 - \alpha = -\varepsilon t^2$.

This equation (B.3) has a symmetry $x \to -x$, hence its spectrum can divided into even and odd parts.

To find a perturbative solution for it, one first solves the auxiliary equation

$$\left(x - \frac{d^2}{dx^2} + t^2\frac{d^4}{dx^4} - t^4\frac{d^6}{dx^6} + \dots\right) F(x) = 0 \tag{B.4}$$

with

$$F(x) = F_0(x) + t^2 F_1(x) + t^4 F_2(x) + \dots$$

The bounded perturbative solution for (B.4) is

$$F(x) = \mathrm{Ai}(x) + \frac{t^2}{5}\left(4x\,\mathrm{Ai}(x) + x^2\,\mathrm{Ai}'(x)\right) + \\ + t^4\left[\left(\frac{x^5}{50} + \frac{5x^2}{7}\right)\mathrm{Ai}(x) + \left(\frac{9x^3}{35} + \frac{6}{35}\right)\mathrm{Ai}'(x)\right] + \dots \tag{B.5}$$

The following two claims provide both the solutions for (B.3) and the spectra for even and odd sectors. In each case we assume that $F(x)$ is the perturbative solution (B.5) for (B.4).

Claim 1. $\psi_{odd}(x) = \operatorname{sign} x\ F(|x| - \varepsilon)$ provides the odd perturbative solution of (B.3) if $F(x)$ is such that

$$\begin{aligned} &F(-\varepsilon) = O(t^2), \\ &F(-\varepsilon) - t^2 F''(-\varepsilon) = O(t^4), \\ &F(-\varepsilon) - t^2 F''(-\varepsilon) + t^4 F^{\mathrm{IV}}(-\varepsilon) = O(t^6). \end{aligned} \tag{B.6}$$

Claim 2. $\psi_{even}(x) = F(|x| - \varepsilon)$ is the even perturbative solution of (B.3) if $F(x)$ satisfies

$$\begin{aligned} &F'(-\varepsilon) = O(t^2), \\ &F'(-\varepsilon) - t^2 F'''(-\varepsilon) = O(t^4), \\ &F'(-\varepsilon) - t^2 F'''(-\varepsilon) + t^4 F^{\mathrm{V}}(-\varepsilon) = O(t^6). \end{aligned} \tag{B.7}$$

The proof of each claim is straightforward. Higher order conditions can be easily written but they are not necessary at the order we are interested in.

In both cases conditions on F, (B.6) and (B.7), are sufficient for determining the spectra. It is easy to check that using them one obtains the following expansion of α in the odd sector

$$\alpha_{odd} = 1 + t^2 z + \frac{t^4 z^2}{5} + t^6\left(-\frac{3}{175}z^3 + \frac{6}{35}\right) + \dots \tag{B.8}$$

and in the even sector

$$\alpha_{even} = 1 + t^2 z + t^4 \left(\frac{z^2}{5} + \frac{1}{5z} \right) + t^6 \left(-\frac{3}{175} z^3 + \frac{3}{25} - \frac{1}{50 z^3} \right) + \dots \tag{B.9}$$

where z is the solution of $\mathrm{Ai}(-z) = 0$ and $\mathrm{Ai}'(-z) = 0$, respectively, thus matching low-energy expansions (2.41) and (2.43) derived above at the chosen order in t.

Appendix C

Computation of $\sigma^{(2)}_{2\to 3}$

As earlier, to simplify notations, we will perform the calculations in the center-of-mass frame, $\theta_1 + \theta_2 = 0$, and set $\theta \equiv \theta_1 - \theta_2 > 0$. It is useful to introduce notations $x = e^{\theta/2}$ and $E = x + x^{-1}$, so that $E = 2\cosh(\theta/2)$ is still the center-of-mass energy in units where $m = 1$. Kinematics demands $E \geqslant 3$, hence $x \geqslant (3+\sqrt{5})/2$.

The relevant matrix element (3.28) in new notations is given now as

$$F(\theta_1, \theta_2|\beta_1, \beta_2, \beta_3) = \bar{\sigma}\,\frac{x^2-1}{x^2+1}\,G(x|\{z_i\}) \tag{C.1}$$

with

$$G(x|\{z_i\}) = \prod_{i<j}^{3}\frac{z_i - z_j}{z_i + z_j}\prod_{i=1}^{3}\frac{x+z_i}{x-z_i}\frac{1+xz_i}{1-xz_i}, \tag{C.2}$$

here $z_i = e^{\beta_i}$. Hence, $\sigma^{(2)}_{2\to 3}$ becomes

$$\sigma^{(2)}_{2\to 3}(\omega) = \frac{2\bar{\sigma}^2}{\pi}\frac{x^2(x^2-1)}{(x^2+1)^3}\;W(x) \tag{C.3}$$

with

$$W(x) = \frac{1}{3!}\int\frac{dz_1}{z_1}\frac{dz_2}{z_2}\frac{dz_3}{z_3}\,\delta(E - \Sigma_i z_i)\delta(E - \Sigma_i 1/z_i)\,G^2(x|\{z_i\}). \tag{C.4}$$

Integration over each z_i goes from 0 to ∞. Since the integral is symmetric with respect to permutations of these variables, we integrate over $0 < z_1 < z_2 < z_3 < \infty$ eliminating the factorial factor. The integral can be further simplified by introducing the symmetric variables

$$s_1 = z_1 + z_2 + z_3, \quad s_2 = z_1z_2 + z_2z_3 + z_1z_3, \quad s = z_1z_2z_3. \tag{C.5}$$

The jacobian of the transformation is

$$D = \left|\frac{\partial(s_1, s_2, s)}{\partial(z_1, z_2, z_3)}\right| = (z_2 - z_1)(z_3 - z_1)(z_3 - z_2) = \\ = \sqrt{s_1^2s_2^2 - 4ss_1^3 - 4s_2^3 + 18ss_1s_2 - 27s^2}. \tag{C.6}$$

In variables s delta-functions become $\delta(E-s_1)$ and $\delta(E-s_2/s)$, thus, integration sets $s_1=E$, $s_2=sE$. The jacobian becomes

$$D\equiv D(E|s)=2E^{3/2}\sqrt{s(s_+-s)(s-s_-)} \tag{C.7}$$

with $s_\pm$ being the ordered solutions, $s_+>s_-$, of the quadratic equation

$$s^2-\frac{E^4+18E^2-27}{4E^3}s+1=0. \tag{C.8}$$

Notice that for $E\geqslant 3$ both roots are real and positive becoming equal at $E=3$, the three-particle threshold.

In new variables $G(x|\{z_i\})$ is

$$G(x|\{z_i\})=G(E|s)=\frac{2E^2+1}{E^2-1}\frac{R(E|s)}{Q(E|s)}\frac{D(E|s)}{s} \tag{C.9}$$

with

$$R(E|s)=s^2+\frac{E(4E^2-7)}{2E^2+1}\,s+1,\quad Q(E|s)=s^2-Es+1. \tag{C.10}$$

Hence, the integral (C.4) becomes

$$W(x)=\int_{s_-}^{s_+}ds\;\frac{G^2(E|s)}{D(E|s)}. \tag{C.11}$$

To simplify further analysis, it is useful to make projective transformation of the integration variable to bring the limits to -1 and 1. We define

$$q=q(E)=\left(\frac{s_+-1}{s_++1}\right)^2=\frac{(E+1)(E-3)^3}{(E-1)(E+3)^3}, \tag{C.12}$$

and introduce t

$$t=\frac{1}{q}\frac{1-s}{1+s}. \tag{C.13}$$

This brings (C.11) to the form

$$W(E)=\frac{2(E+2)^2(2E-1)^4(E-3)^3}{(E-2)^2(E^2-1)(E+3)^{3/2}(E-1)^{3/2}}\times \\ \times\int_{-1}^{1}dt\,\frac{\sqrt{1-t^2}}{(1-q\,t^2)^{3/2}}\left(\frac{1-\mu\,t^2}{1-\nu\,t^2}\right)^2 \tag{C.14}$$

with

$$\mu=q\,\frac{(E-2)(2E+1)^2}{(E+2)(2E-1)^2},\quad \nu=q\,\frac{E+2}{E-2}. \tag{C.15}$$

Finally, collecting everything together we come to the expression (3.35)

$$\sigma^{(2)}_{2\to 3} = N(E)I(E) \tag{C.16}$$

with

$$I(E) = \int_{-1}^{1} dt\, \frac{\sqrt{1-t^2}}{(1-q\,t^2)^{3/2}} \left(\frac{1-\mu\,t^2}{1-\nu\,t^2}\right)^2 \tag{C.17}$$

and

$$N(E) = \frac{4\bar{\sigma}^2}{\pi} \frac{(E+2)^{5/2}}{(E-2)^{3/2}} \frac{(E-3)^3(2E-1)^4}{(E+3)^{3/2}(E-1)^{5/2}(E+1)E^3}. \tag{C.18}$$

We can use now this expression to study behavior of the $\sigma^{(2)}_{2\to 3}$ at the threshold and high energies.

Appendix D

Near-threshold behavior of $\sigma^{(2)}_{2\to n}$

Here we compute the main leading term in $\sigma^{(2)}_{2\to n}$ near the threshold $E \to n$.

In the center-of-mass frame we have

$$P_{in} = (E, 0), \quad P_{out} = (\Sigma_i \cosh\beta_i, \Sigma_i \sinh\beta_i)\,. \tag{D.1}$$

Using the expression for the matrix element (3.28), we get

$$\sigma^{(2)}_{2\to n}(w) = \frac{2\sqrt{E^2-4}}{E^3}\frac{\bar\sigma^2}{n!}\int\left[\prod_{i=1}^n \frac{d\beta_i}{2\pi}\right](2\pi)^2\delta\left(E-\Sigma_i\cosh\beta_i\right)\delta\left(\Sigma_i\sinh\beta_i\right)\times \\ \times\prod_{i=1}^n\left(\frac{E+2\cosh\beta_i}{E-2\cosh\beta_i}\right)^2\prod_{j>i=1}^n\tanh^2\frac{\beta_i-\beta_j}{2}. \tag{D.2}$$

We are interested in the threshold behavior $E = n + \varepsilon$ with $\varepsilon \to 0_+$. In this limit, all β_i are small so that the integral is simplified

$$\sigma^{(2)}_{2\to n}(w) = \frac{2\sqrt{E^2-4}}{E^3}\frac{\bar\sigma^2}{2^{n^2-n}}\left(\frac{E+2}{E-2}\right)^{2n} W_n(E), \tag{D.3}$$

where

$$W_n(E) = \frac{1}{n!}\int\left[\prod_{i=1}^n\frac{d\beta_i}{2\pi}\right](2\pi)^2\delta\left(\varepsilon-\Sigma_i\beta_i^2/2\right)\delta\left(\Sigma_i\beta_i\right)\Delta^2(\beta) \tag{D.4}$$

with $\Delta(\beta) = \prod_{i<j}(\beta_i - \beta_j)$ being the Vandermonde determinant.

The integral for $W_n(E)$ is evaluated in the following way. Rewrite $W_n(E)$ as

$$W_n(E) = \int_{-\infty}^{\infty} dt\, e^{-i\varepsilon t} D_n(t) \tag{D.5}$$

with

$$D_n(t) = \int_{-\infty}^{\infty} dx \int\left[\prod_{i=1}^n\frac{d\beta_i}{2\pi}\right] e^{i\sum_i\left(t\beta_i^2/2+x\beta_i\right)}\Delta^2(\beta). \tag{D.6}$$

Using the shift, $\beta_i = y_i - x/t$, one obtains for $D_n(t)$

$$D_n(t) = \sqrt{\frac{2\pi t}{in}}\int\left[\prod_{i=1}^n\frac{dy_i}{2\pi}\right] e^{it\sum_i y_i^2/2}\Delta^2(y). \tag{D.7}$$

Another change of variables, $y_i = z_i\sqrt{i/t}$, gives

$$D_n(t) = \sqrt{\frac{2\pi}{n}}\left(\frac{i}{t}\right)^{(n^2-1)/2}\int\left[\prod_{i=1}^{n}\frac{dz_i}{2\pi}\right]e^{-\sum_i z_i^2/2}\Delta^2(z). \tag{D.8}$$

The integral over z_i is evaluated in closed form [42]

$$\int\left[\prod_{i=1}^{n}\frac{dz_i}{2\pi}\right]e^{-\sum_i z_i^2/2}\Delta^2(z) = \frac{\prod_{p=1}^{n}p!}{(2\pi)^{n/2}}. \tag{D.9}$$

Hence, for $W_n(E)$ we have

$$W_n(E) = \frac{\prod_{p=1}^{n-1}p!}{\sqrt{n}}\frac{i^{(n^2-1)/2}}{(2\pi)^{(n-1)/2}}\int_{-\infty}^{\infty}dt\,\frac{e^{-i\varepsilon t}}{(t^2+i0)^{(n^2-1)/2}} = \\ = \frac{\prod_{p=1}^{n-1}p!}{\sqrt{n}}\frac{(E-n)^{(n^2-3)/2}}{(2\pi)^{(n-3)/2}\,\Gamma\left(\frac{n^2-1}{2}\right)}. \tag{D.10}$$

Collecting everything and keeping the leading term, we get the threshold behavior (3.41).

Vita

Iskander Ziyatdinov

Degrees

2002	Master of Science in Physics, Moscow State University, Moscow, Russia
2011	Ph.D. in Physics, Rutgers University, New Brunswick, New Jersey, USA

Positions held

2004-2006	Graduate Fellow, Rutgers University
2006-2011	Teaching and Research Assistant, Rutgers University

Publications

2003	"Parquet approximation for large N matrix Higgs model" with A. Shishanin, JHEP 0307 (2003) 032; hep-th/0303169.
2005	"Parquet approximation for two-matrix model," Moscow State University Bulletin, 5 (2005) 7.
2010	"Asymptotic properties of mass spectrum in 't Hooft's model of mesons," Int. J. Mod. Phys. **A** 25 (2010) 3899; arXiv:1003.4304.
2011	"Inelastic scattering and elastic amplitude in Ising field theory in a weak magnetic field at $T > T_c$. Perturbative analysis." with A. Zamolodchikov, arXiv:1102.0767.